

AD-A270 893



NRL/FR/7142--93-9570

Measurements of Ocean Surface and Bottom Backscattering Strengths in the Northwestern Atlantic Ocean

NOLAN R. DAVIS
JOSEPH JEFFERY
FRED T. ERSKINE

*Acoustic Systems Branch
Acoustics Division*

October 8, 1993



Approved for public release; distribution unlimited.

251
950

93-24125



REPORT DOCUMENTATION PAGE			Form Approved OMB No. 0704-0188										
<small>Public reporting burden for this collection of information is estimated to average 1 hour per response, including the time for reviewing instructions, searching existing data sources, gathering and maintaining the data needed, and completing and reviewing the collection of information. Send comments regarding this burden estimate or any other aspect of this collection of information, including suggestions for reducing this burden, to Washington Headquarters Services, Directorate for Information Operations and Reports, 1215 Jefferson Davis Highway, Suite 1204, Arlington, VA 22202-4302, and to the Office of Management and Budget, Paperwork Reduction Project (0704-0188), Washington, DC 20503.</small>													
1. AGENCY USE ONLY (Leave Blank)		2. REPORT DATE October 8, 1993		3. REPORT TYPE AND DATES COVERED Final									
4. TITLE AND SUBTITLE Measurements of Ocean Surface and Bottom Backscattering Strengths in the Northwestern Atlantic Ocean			5. FUNDING NUMBERS PE - 62435N PR - R035B03										
6. AUTHOR(S) Nolan R. Davis, Joseph Jeffery, and Fred T. Erskine													
7. PERFORMING ORGANIZATION NAME(S) AND ADDRESS(ES) Naval Research Laboratory Washington, DC 20375-5320			8. PERFORMING ORGANIZATION REPORT NUMBER NRL/FR/7142-93-9570										
9. SPONSORING/MONITORING AGENCY NAME(S) AND ADDRESS(ES) Office of Naval Research Arlington, VA 22217-5000			10. SPONSORING/MONITORING AGENCY REPORT NUMBER										
11. SUPPLEMENTARY NOTES													
12a. DISTRIBUTION/AVAILABILITY STATEMENT Approved for public release; distribution unlimited.			12b. DISTRIBUTION CODE										
13. ABSTRACT (Maximum 200 words) <p>Experimental measurements of ocean surface and bottom backscattering strengths were carried out in the northwestern Atlantic Ocean during July and August 1990. The experiment used ship and air deployed explosive charges to provide ensonification of the ocean surface and bottom over a range of low frequencies up to 1 kHz. Overall, the surface backscatter results agreed well with the Ogden-Erskine curves, matching the predicted dependence on wind speed, grazing angle, and frequency. At two sites northeast of the Grand Banks, the surface backscattering strengths appeared to be dominated by volume backscattering caused by fish. The bottom backscattering strengths were observed to have considerable variation in level (up to 17 dB) between different sites. As a function of grazing angle, most of the bottom backscattering strength curves paralleled the Mackenzie curve for grazing angles between 30° and 50°. A moderate frequency dependence of approximately 3 dB was observed. Comparisons of the bottom backscattering strengths with the Damuth 3.5 kHz echo-character province types yielded no consistent correlations. Comparisons with archival results for the same region yielded general agreement within 6 dB. Comparison of the ship-based and airborne techniques showed that they yielded comparable backscattering strengths to within 5 dB.</p>													
14. SUBJECT TERMS <table border="0"> <tr> <td>Surface scattering</td> <td>Grazing angle</td> <td>Ogden-Erskine</td> </tr> <tr> <td>Volume scattering</td> <td>Wind speed</td> <td>Mackenzie</td> </tr> <tr> <td>Bottom scattering</td> <td>Chapman-Harris</td> <td>Damuth</td> </tr> </table>			Surface scattering	Grazing angle	Ogden-Erskine	Volume scattering	Wind speed	Mackenzie	Bottom scattering	Chapman-Harris	Damuth	15. NUMBER OF PAGES 59	
Surface scattering	Grazing angle	Ogden-Erskine											
Volume scattering	Wind speed	Mackenzie											
Bottom scattering	Chapman-Harris	Damuth											
			16. PRICE CODE										
17. SECURITY CLASSIFICATION OF REPORT UNCLASSIFIED		18. SECURITY CLASSIFICATION OF THIS PAGE UNCLASSIFIED		19. SECURITY CLASSIFICATION OF ABSTRACT UNCLASSIFIED									
			20. LIMITATION OF ABSTRACT UL										

CONTENTS

INTRODUCTION	1
BACKGROUND	4
EXPERIMENTAL GEOMETRY AND TECHNIQUE	4
DATA ANALYSIS	5
SURFACE BACKSCATTERING RESULTS	7
BOTTOM BACKSCATTERING RESULTS	8
Grazing Angle Dependence of Bottom Backscattering Strengths	8
Frequency Dependence of Bottom Backscattering Strengths	14
Comparisons with Archival Results	22
COMPARISON OF EXPERIMENTAL TECHNIQUES	23
Comparison Between Ship-Based and Airborne Techniques	23
Merging vs Averaging in Scattering Strength Computations	23
SUMMARY AND CONCLUSIONS	30
Surface Backscattering Strengths	34
Bottom Backscattering Strengths	34
Comparison of Experimental Techniques	34
ACKNOWLEDGMENTS	35
REFERENCES	35
APPENDIX A - Calibration for the NRL Towed Line Array Processing System	37
APPENDIX B - Representative Sound Speed Profiles	41
APPENDIX C - 3.5 kHz Echo Sounder Plots	45

Accession For	
NTIS CRA&I	<input checked="" type="checkbox"/>
DTIC TAB	<input type="checkbox"/>
Unannounced	<input type="checkbox"/>
Justification _____	
By _____	
Distribution / _____	
Availability Codes	
Dist	Avail and/or Special
A-1	

MEASUREMENTS OF OCEAN SURFACE AND BOTTOM BACKSCATTERING STRENGTHS IN THE NORTHWESTERN ATLANTIC OCEAN

INTRODUCTION

Measurements of ocean surface and bottom backscattering strengths were conducted in the northwestern Atlantic Ocean during July and August 1990. The test consisted of two separate experiment cruises. The first was part of a joint U.S.-Canadian exercise carried out as a collaboration between the U. S. Naval Research Laboratory (NRL) and the Canadian Defence Research Establishment Atlantic (DREA). This experiment cruise, referred to in this document as NRL Cruise 709-90, took place in two main areas, one approximately 1000 km northeast of the Grand Banks and the other approximately 450 km southeast of the Grand Banks. The second experiment cruise, referred to as NRL Cruise 710-90, was conducted by NRL and took place approximately 250 km south of Nova Scotia. The primary research platform for both experiments was the research vessel USNS *Lynch*, which deployed a towed horizontal line array receiver. In addition, a Navy P-3 aircraft was used in both experiments to provide further coverage of test sites and to conduct acoustic backscattering measurements for comparison with ship-based measurements at identical sites. Figure 1 shows the locations of the experimental sites, and Table 1 gives the geographic coordinates and relevant environmental parameters. Airborne Flights c1, c2, and d were components of Cruise 709-90, while Flights f, g, h, and j were components of Cruise 710-90. In all, backscattering strength data were collected and analyzed for 7 runs from Cruise 709-90, 4 runs from Cruise 710-90, and 7 aircraft flights.

The primary objective of the experiments was to measure the ocean surface and bottom backscattering strengths and to characterize their dependence on environmental parameters. Specifically, the experiments examined the dependence of surface backscattering strengths on wind speed, grazing angle, and frequency. They examined the dependence of bottom backscattering strengths on bottom grazing angle and frequency as well as any known geophysical information. The range of environmental parameters included wind speeds between 1.0 and 12.3 m/s and bottom depths between 2215 and 4790 m. Bottom grazing angles down to 30° were achieved.

In addition to the basic scientific objectives, the analysis also examined certain aspects of the experimental technique itself. It compared differences between using a horizontal line array and omnidirectional sonobuoys as receivers, and it examined two different methods of combining the data from multiple trials to obtain backscattering strengths.

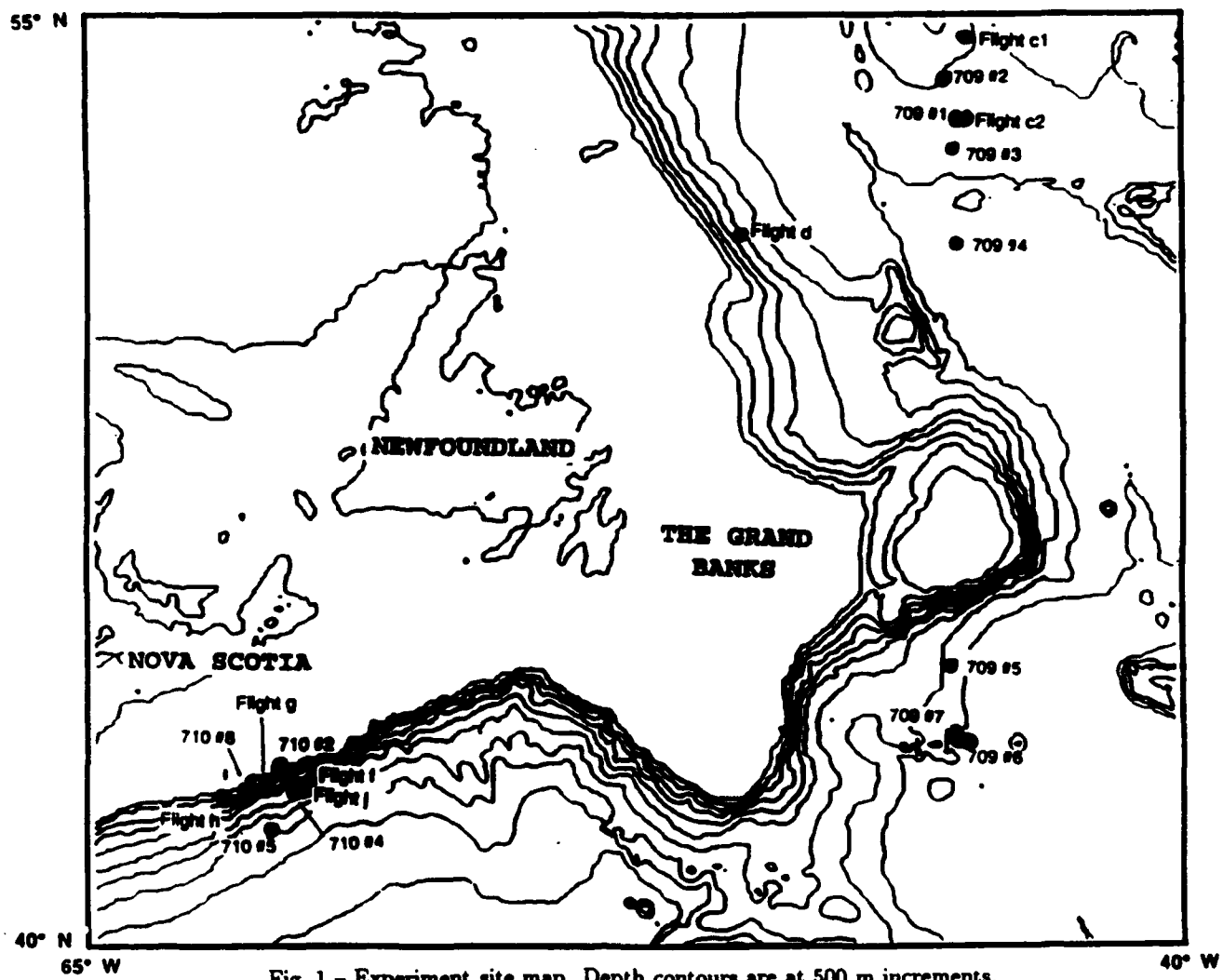


Fig. 1 - Experiment site map. Depth contours are at 500 m increments.

Table 1 - Experiment Sites

RUN	Latitude	Longitude	Wind Speed (m/s)	Bottom Depth (m)	Damuth Province Type
709-1	53° 15.9' N	45° 01.5' W	3.1	3940	IA
709-2	53° 53.1' N	45° 20.8' W	6.2	3590	V
709-3	52° 48.6' N	45° 00.0' W	12.3	3960	IA
709-4	51° 14.6' N	45° 00.7' W	9.3	4125	General
709-5	44° 37.0' N	45° 09.4' W	4.1	4210	IIA
709-6	43° 20.5' N	44° 35.5' W	4.1	4790	General
709-7	43° 24.5' N	44° 46.6' W	4.1	3200	IIA
710-2	42° 56.2' N	60° 41.7' W	4.1	2215	Unknown
710-4	42° 26.8' N	60° 17.7' W	3.6	3750	IA
710-5	41° 54.9' N	60° 48.5' W	1.0	4175	V
710-8	42° 32.8' N	61° 18.6' W	6.7	2775	IA
709 Flight c1	54° 30.0' N	45° 00.0' W	5.6	3628	V
709 Flight c2	53° 09.6' N	45° 00.0' W	6.7	3838	IA
709 Flight d	51° 36.8' N	45° 04.0' W	5.4	4134	Unknown
710 Flight f	42° 40.6' N	60° 01.3' W	3.1	3654	General
710 Flight g	42° 42.8' N	60° 47.2' W	2.9	2945	IA
710 Flight h	42° 20.7' N	61° 42.2' W	2.7	2893	IA
710 Flight j	42° 33.1' N	60° 10.5' W	3.8	3682	General

BACKGROUND

Determination of ocean surface and bottom backscattering strengths is important for understanding long-range reverberation in the ocean. This is particularly important at low frequencies (below 1 kHz) for which reverberation from surface and bottom backscatterers at long ranges may significantly limit the performance of active sonar systems.

In recent decades, the sea surface backscattering strengths used for sonar performance modeling have often been based on empirical results obtained by Chapman and Harris [1] and Chapman and Scott [2], who measured surface backscattering strengths as a function of wind speed, grazing angle, and frequency. They then fitted these data with simple empirical formulas, referred to as the Chapman-Harris curves. It is now known that these curves, when extrapolated to low-wind, low-frequency, and low-sea conditions, significantly underestimate the observed backscattering strengths. Attempts have been made to predict the backscattering strengths in these conditions using first-order perturbation theory for rough surfaces (e.g., see Ref. 3). These efforts have been moderately successful in the low-wind, high-frequency regime. More recently a comprehensive series of experiments which cover a wide range of wind and sea conditions have been carried out by Ogden and Erskine [4]. The analysis of these results has resulted in an empirical algorithm for predicting surface backscattering strengths in a broad range of frequencies and wind speeds. This algorithm appears to bridge successfully the gap between the predictions of perturbation theory that are valid in the low-wind, high-frequency regime and the predictions of Chapman and Harris that are valid in the high-wind regime.

Estimates of bottom backscattering strengths used in sonar performance predictions are often based on Lambert's rule, which asserts that the backscattered intensity is proportional to the product of the sine of the incident grazing angle and the sine of the backscattering grazing angle. The utility of this description was first reported by Mackenzie [5]. When the constant of proportionality is chosen to be -27 dB, this rule is often called the Mackenzie curve. However this simple description has met with limited success, particularly because of its lack of dependence on frequency and geophysical bottom parameters. Much experimental work has been done recently to obtain bottom backscattering strength data over a large range of bottom types. To date, however, there is no consistent framework for classifying or predicting bottom backscattering strengths on the basis of measured bottom parameters.

EXPERIMENTAL GEOMETRY AND TECHNIQUE

The experiment used two modes of data collection: ship-based and airborne. The ship-based data collection used as its receiver a horizontal towed line array at a depth of approximately 70 m. The array hydrophone spacing was 1.25 m, giving a nominal design frequency of 600 Hz. The tow ship speed was approximately 1.5 m/s. The towed array data were digitized with a sampling rate of 2560 Hz for the Cruise 709 data and 2048 Hz for the Cruise 710 data. The data were recorded on a high-density digital recorder (HDDR) for subsequent postprocessing at NRL.

The experiment used explosive charges to generate acoustic energy in the water over a broad frequency range (0 to 1 kHz). These charges were Mk61 SUS (Signals, Underwater Sound), which contain 0.82 kg (1.8 lb) of TNT and are detonated by a pressure-activated device at 244 m. Drag plates were attached to the SUS to give a rate of descent such that detonation occurred approximately

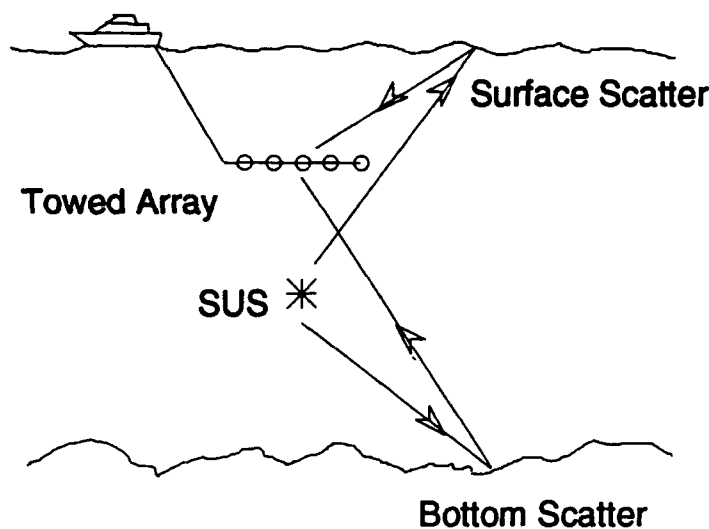


Fig. 2 - Experiment geometry for ship-based technique

directly beneath the towed line array receiver. This geometry is referred to as “quasi-monostatic” (Fig. 2) because of the relatively small vertical separation between source and receiver and essentially zero horizontal separation. By measuring the direct path reverberation levels at the receiver after single interactions with the backscattering surface, knowing the source level, modeling the propagation from the source to the backscatterer and back to the receiver, and estimating the geometric backscattering patch areas, one can calculate the ocean surface and bottom backscattering strengths.

The airborne technique used AN/SSQ-57A sonobuoys for omnidirectional receivers, deployed at a depth of 122 m. At each site, a suite of sonobuoys with different attenuations (0, 20, and 40 dB, or 20, 40, and 60 dB) were deployed from a Navy P-3 aircraft to allow measurement of the full dynamic range of the reverberation time series without saturation and above the sonobuoy sensitivity limit. The aircraft dropped the sonobuoys as close to each other as possible and then flew a “90-270” pattern (shaped like a barbell or figure eight) to deploy the SUS at the crossover point above the sonobuoys to give a nearly quasi-monostatic geometry (Fig. 3). The collected data were transmitted by radio to the aircraft and recorded on an analog recorder. At NRL, the data were filtered and digitized with a sampling rate of 2 kHz. Horizontal source-receiver separation distance was estimated by measuring the delay between the direct arrival and the surface return, given an assumed depth of detonation of the SUS. Among the data collected, the average horizontal source-receiver separation was approximately 0.5 km.

DATA ANALYSIS

The data were analyzed at frequencies corresponding to the harmonics of the SUS explosive pulse bubble frequency, which was approximately 54 Hz for Mk61 SUS detonated at 244 m. Reverberation levels were averaged over a 10 Hz band centered at the bubble frequency harmonics. Analysis of the ship-based data collected on the towed horizontal line array receiver covered the frequency range 250 to 600 Hz. The lower bound of 250 Hz was imposed to avoid the low frequency rolloff in the towed line array electronic system. The upper limit of 600 Hz was imposed to avoid

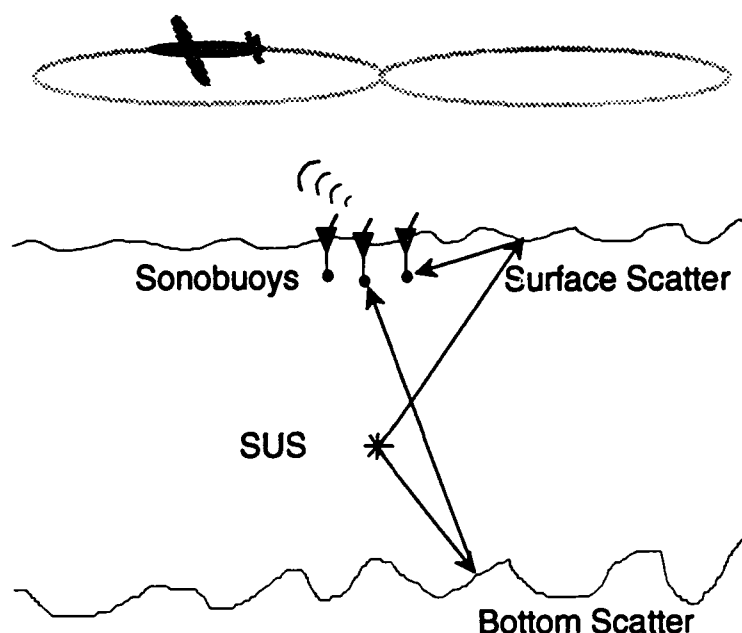


Fig. 3 - Experiment geometry for airborne technique

aliasing on the towed line array. Analysis of the airborne data collected on the omnidirectional sonobuoys covered the frequency range 250 to 1000 Hz, with the upper limit of 1000 Hz being the Nyquist rate for the airborne data sampling rate of 2 kHz.

The backscattering strength analysis was performed using the Direct Path (DP) analysis software developed at NRL [6]. This software package used a ray trace to compute propagation loss from the source to the backscatterer and back to the receiver [7]. The ray trace calculation incorporated on-site estimates of the water depth, as well as sound speed profile information obtained from *in situ* bathythermograph measurements. The acoustic data were Fourier analyzed in 0.25 s increments using a Hamming-shaded temporal window, with 50% overlap between adjacent windows. The geometry of the calculation assumed a flat interface at the ocean surface and ocean bottom, so that the ensonified area for each 0.25 s increment corresponded to an elliptical annulus on the interface surface. For the airborne measurements using omnidirectional receivers, this ensonified area was equal to the calculated backscattering area, whereas, for the ship-based measurements using the towed line array, the calculated backscattering area was represented by the intersections of the backscattering elliptical annuli with the receiver beams (between the 3 dB down points). The mean grazing angle parameter was computed as the average grazing angle over the respective calculated backscattering areas.

In the data processing, individual SUS shots were discarded if the depths of detonation were not consistent with the specified depth, as evidenced by unusual bubble frequency harmonics, or if the horizontal source-receiver separations were too large or not consistent with the majority of the shots. Once an ensemble of "good" shots was assembled, generally containing between 6 and 19 shots, the reverberation levels were averaged over this ensemble. Shot-to-shot variability in reverberation levels resulted in an experimental measurement uncertainty of about ± 3 dB. A single set of backscattering strengths was then computed using the merged reverberation levels.

The extraction of the backscattering strengths was based on a sonar equation (e.g., see Ref. 8) that expressed the backscattering strength in terms of the emitted and received sound levels and the propagation physics,

$$SS = RL - SL + TL_{out} + TL_{in} - 10 \log A - 10 \log B, \quad (1)$$

where SS is the backscattering strength in dB, RL is the received level in dB re $(1\mu\text{Pa})^2/\text{Hz}$, SL is the source level in dB re $(1\mu\text{Pa})^2/\text{Hz}$ at 1 m, TL_{out} is the transmission loss in dB from the source to the ensonified area, TL_{in} is the transmission loss in dB from the ensonified area to the receiver, A is the ensonified area of the ocean surface or ocean bottom in m^2 , and B is the effective area in m^2 of the receiver beampattern using a 3 dB down beamwidth. Source levels for the SUS were obtained from curves given by Urlick [9]. Overall uncertainties in the calculated backscattering strengths resulting from the combination of all terms in the sonar equation were typically ± 5 dB.

Beamforming was done on a subarray of 16 hydrophones to form 17 beams using Hamming shading. This size subarray was chosen to ensure that the ocean surface backscattering patch was in the far field of the array. (Since the experiments took place in deep water with depths averaging around 3500 m, the ocean bottom was always in the far field of the array.) Using the far-field criterion $l_o = L^2/\lambda$, where L was the aperture length and λ was the shortest wavelength of interest (in this case at the array design frequency), the far-field distance was $l_o = (15 \cdot 1.25 \text{ m})^2/(1.25 \text{ m}) \approx 280 \text{ m}$. As a result, attention was restricted to surface returns beyond about 0.4 s after the direct arrival, guaranteeing that the surface backscattering regions were in the far field of the array. A subset of the beams (numbered 2 to 12) was used in the analysis of the surface backscattering strengths, giving coverage over angles 20° to 115° relative to aft endfire. The forward and aft endfire beams were not used since good estimates of the beampattern ensonification area were difficult to obtain. Moreover, the forward-most beams were omitted to suppress ownship noise. For calculating the bottom backscattering strengths, only beams numbered 2 to 5, with coverage over angles 20° to 70° relative to aft endfire, were used in order to suppress fathometerlike returns in the broadside beams that tended to contaminate the backscattering strength data for higher grazing angles (generally above 40° mean grazing angle).

Appendix A describes the calibration used for the ship-based processing. If alternate possible calibration values were used, the ship-based backscattering strengths in this report would be adjusted upward by 1 to 5 dB. Such a change would not affect the backscattering strengths obtained from the airborne data.

SURFACE BACKSCATTERING RESULTS

The primary objective of the surface backscattering measurements was to characterize surface backscattering strengths as a function of wind speed, grazing angle, and frequency. During the experiment, wind speeds were measured with an anemometer on a mast at an approximate height of 15 m above sea level and adjusted for relative ship speed. Data were collected and processed for all the Cruise 709, Cruise 710, and airborne sites. However, the processing of the airborne surface backscatter data did not yield reliable results.

Overall, the measured grazing angle dependence of the surface backscatter, as parameterized by frequency and wind speed, was consistent with the Ogden-Erskine curves. As an example of these

results, Fig. 4 shows surface backscattering strength plotted as a function of mean grazing angle for seven frequencies between 250 and 550 Hz (dotted lines) for Run 710-4a. The Ogden-Erskine curves for the measured wind speed of 3.6 m/s are shown on the same plot (solid lines). The measured results were in reasonable agreement with the predictions of the Ogden-Erskine curves. Note that at this low wind speed the backscattering strengths showed little dependence on frequency.

Figures 5 and 6 present surface backscattering strengths for Runs 709-1 and 709-2, which were located northeast of the Grand Banks. The test times were late afternoon to early evening (1600-1825 and 1855-1950 local time, respectively). The solid lines represent the Ogden-Erskine curves for the measured wind speeds of 3.1 and 6.2 m/s, respectively. At these sites, the surface backscattering results appeared to be dominated by volume backscattering caused by fish, as evidenced by a lack of dependence of the backscattering strengths on grazing angle. This characteristic flattening of measured surface backscattering strengths at low grazing angles resulting from the presence of fish scatterers has been reported by other NRL investigators (e.g., see Ref. 10).

BOTTOM BACKSCATTERING RESULTS

The primary objective of the bottom backscattering experiment was to characterize the bottom backscattering strengths as a function of grazing angle, frequency, and any known geophysical parameters of the experimental sites.

Grazing Angle Dependence of Bottom Backscattering Strengths

Figures 7 and 8 present measured backscattering strengths as a function of grazing angle at 250 and 550 Hz for all the Cruise 709 ship-based sites. The smooth solid line in all the bottom backscattering strength plots is the Mackenzie curve. Also, the notations a, b, and c denote different segments of the same run at the same site, with approximately 10 SUS shots per segment.

At 250 Hz the data curves of Fig. 7 appeared to fall into two groups: The first group, containing Runs 709-2, 709-3, 709-4, 709-5a, and 709-5b, were from sites in the Gloria Drift and the southern end of the Labrador Basin. They generally followed the Mackenzie curve but were about 6 dB above it. The second group, containing Runs 709-6b, 709-6c, and 709-7, were from sites located in the Newfoundland Basin. They were flatter than the Mackenzie curve for grazing angles below 40° and were 12 to 14 dB above it around 30° grazing angle. (Run 709-6a was omitted since it occurred over the slope of a steep seamount.) As a special case, it should be noted that Run 709-7 was directly above an isolated seamount, which may account for the anomalously large backscattering strengths around 44° grazing angle, but may also make the calculation suspect because of violation of the flat-bottom assumption. At 550 Hz the results of Fig. 8 were similar, but with a few notable exceptions. Runs 709-3 and 709-5a backscattering strengths stayed rather low between grazing angles 43° and 60°. Runs 709-6b, 709-6c, and 709-7 backscattering strength curves approximately paralleled the Mackenzie curve for grazing angles below 40° at this frequency. The anomalously high backscattering strengths for Run 709-7 were absent. Also note that the Run 709-5b values were consistently about 4 dB higher than the Run 709-5a values, even though they were from the same site. This result suggests a range variability of as much as 4 dB over distances of about 4.2 km. Another notable feature is that Runs 709-2 and 709-3 showed a 4 dB spike at 37° grazing angle.

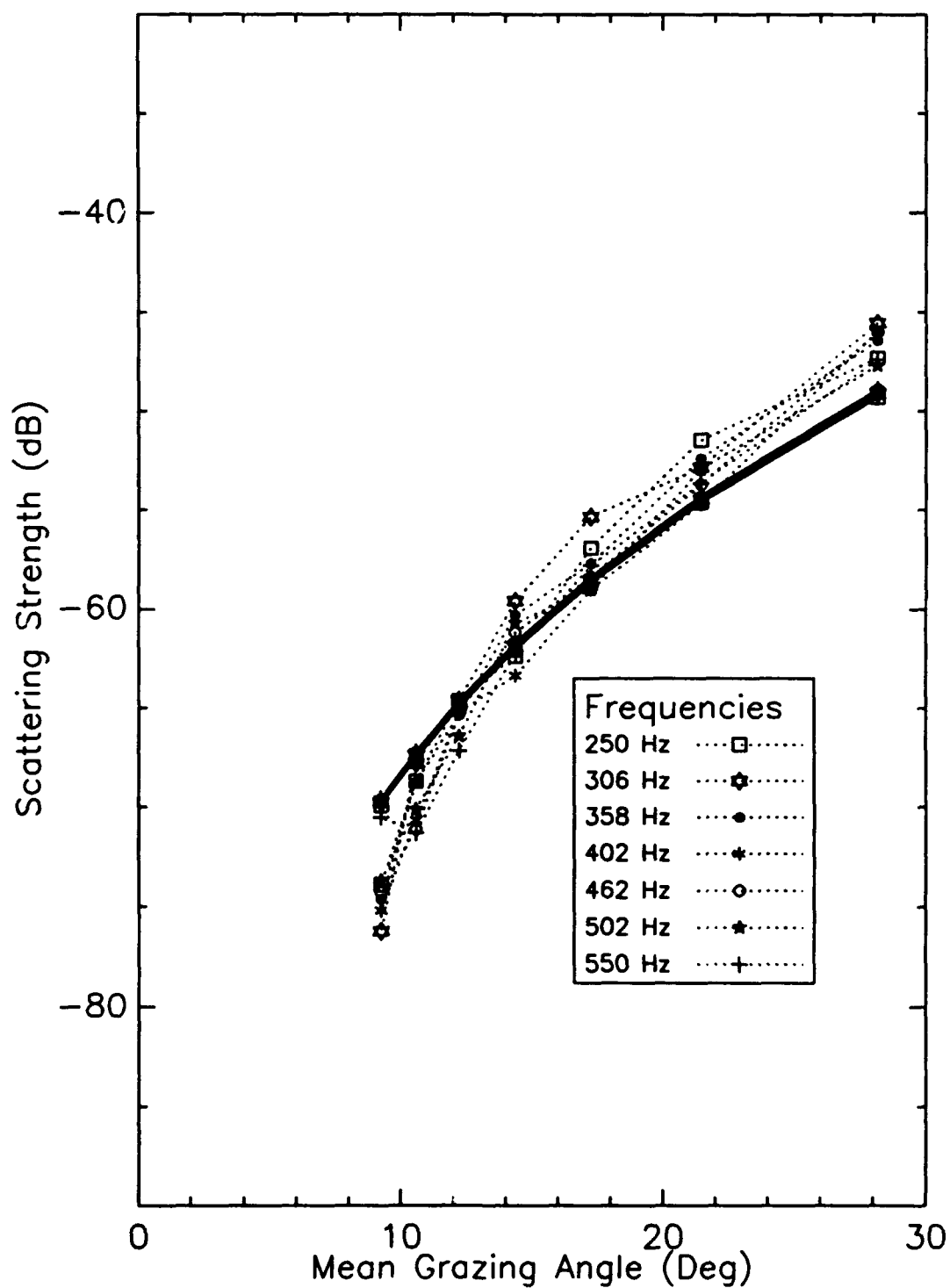


Fig. 4 - Surface backscattering strengths for Run 710-4a. The solid lines represent the Ogden-Erskine curves for a wind speed of 3.6 m/s.

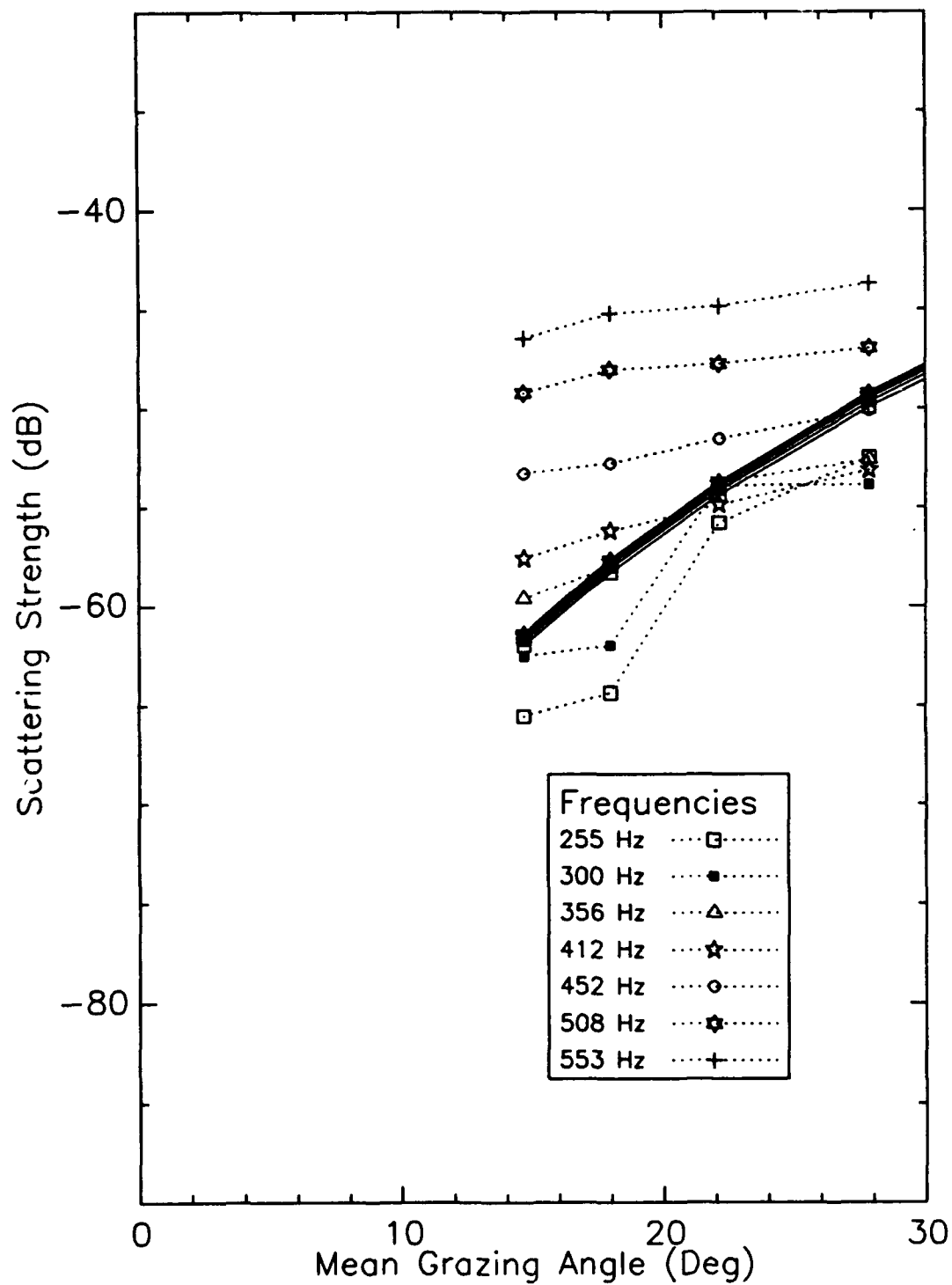


Fig. 5 - Surface backscattering strengths for Run 709-1. The solid lines represent the Ogden-Erskine curves for a wind speed of 3.1 m/s.

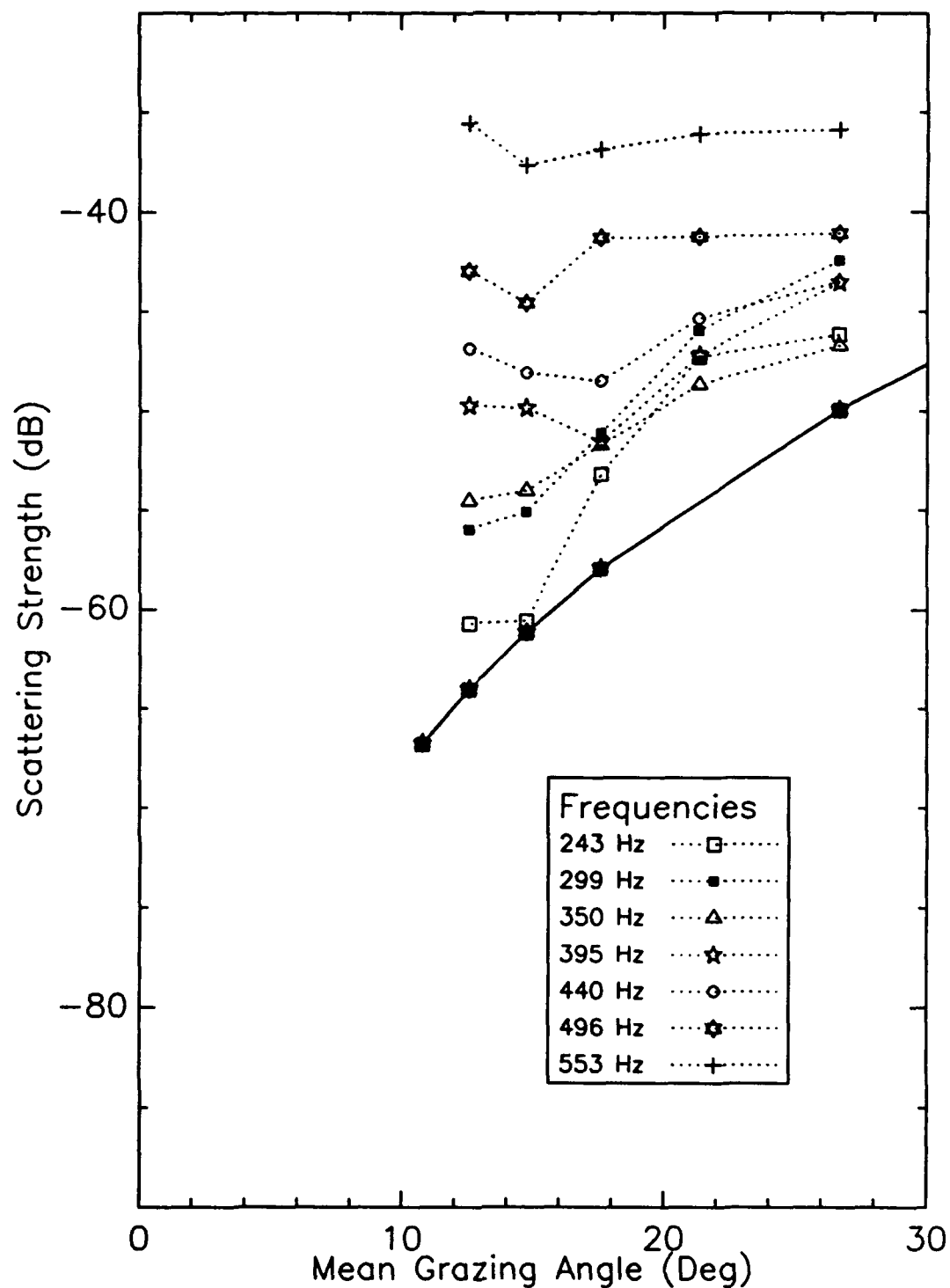


Fig. 6 - Surface backscattering strengths for Run 709-2. The solid lines represent the Ogden-Erskine curves for a wind speed of 6.2 m/s.

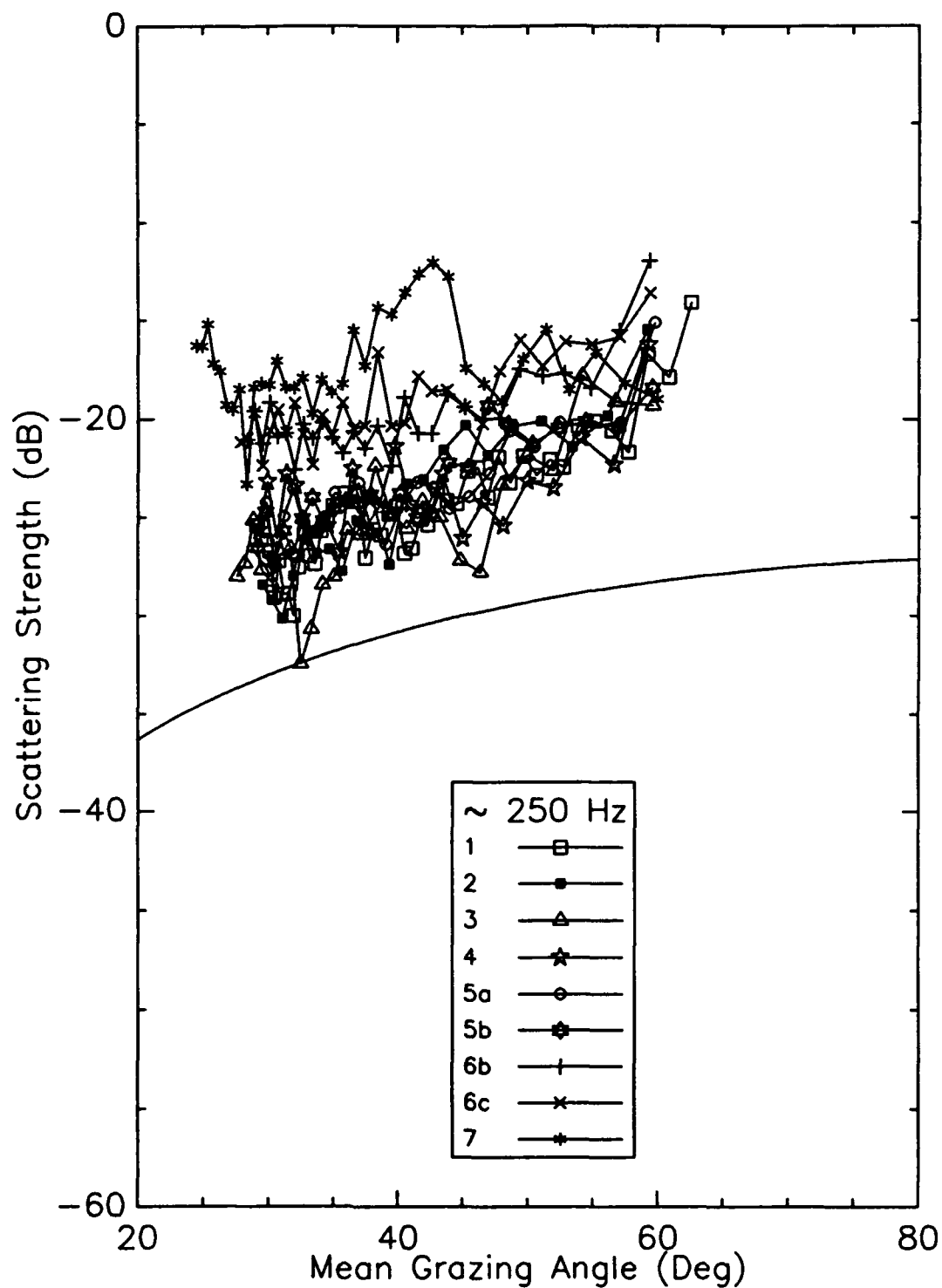


Fig. 7 - Grazing angle dependence of bottom at 250 Hz for all Cruise 709 ship-based sites. The smooth solid line is the Mackenzie curve.

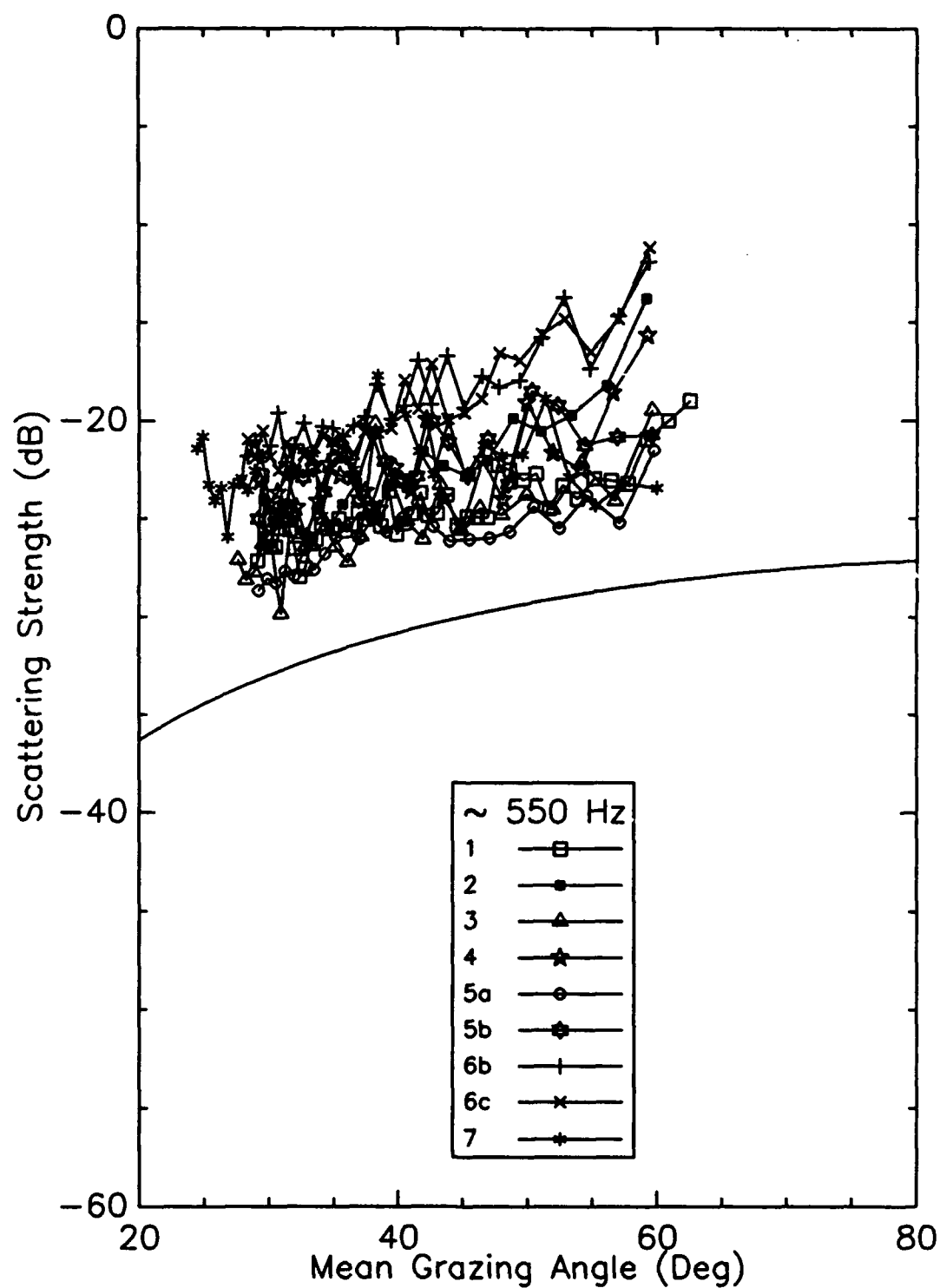


Fig. 8 - Grazing angle dependence of bottom backscattering strengths at 550 Hz for all Cruise 709 ship-based sites. The smooth solid line is the Mackenzie curve.

Figures 9 and 10 present backscattering strengths as a function of grazing angle at 250 and 550 Hz for the Cruise 710 sites, all of which were located on the continental rise south of Nova Scotia. There were loosely three sets of backscattering strength curves. One set, containing Runs 710-2 and 710-8, roughly followed the Mackenzie curve but about 2 dB above it. Another set, containing Runs 710-4a and 710-4b, were flatter than the Mackenzie curve at grazing angles below 40° and were 2 to 4 dB below it. Differences between Runs 710-4a and 710-4b suggest a same-site local variability in backscattering strength of around 4 dB. The remainder was Run 710-5, which was approximately 9 dB above and parallel to the Mackenzie curve at 250 Hz, but 6 dB above and flatter than the Mackenzie curve at 550 Hz.

Figures 11 and 12 present backscattering strengths as a function of grazing angle at 506 and 910 Hz for the Cruise 709 and 710 airborne SUS experiment sites. In these results there was a clustered group of curves, containing Flights d, f, g, and h, that was approximately 2 dB below and parallel to the Mackenzie curve. The Flight d site was on the continental rise east of Newfoundland, while the Flight f, g, and h sites were on the continental rise south of Nova Scotia. The backscattering strength curve for the Flight c2 site, located between the Gloria Drift and the Newfoundland continental rise, also paralleled the Mackenzie curve but about 5 dB above it, whereas the backscattering strength curve for the Flight j site, located on the continental rise south of Nova Scotia, paralleled the Mackenzie curve but about 5 dB below it. The remaining Flight c1 site was unique in that the backscattering strengths were essentially independent of grazing angle. Note that Flights c1 and c2 were not adjacent but rather were separated by approximately 19 km.

Frequency Dependence of Bottom Backscattering Strengths

The Mackenzie curve does not predict any frequency dependence for bottom backscattering strengths. Experimentally, however, frequency dependence is generally observed, and the character of this dependence can change between different sites.

Figures 13, 14, and 15 present bottom backscattering strengths as a function of frequency at a fixed average grazing angle of 32° for, respectively, the Cruise 709 ship-based sites, Cruise 710 ship-based sites, and Cruise 709 and 710 airborne sites. The values shown are local averages of the backscattering strengths in dB over five data points having grazing angles close to 32° (generally within $\pm 2^\circ$). For reference, the Mackenzie curve gives a value of -32.5 dB at 32° grazing angle.

Analysis of the frequency dependence of the Cruise 709 data at 32° grazing angle (Fig. 13) showed two basic groupings of backscattering strengths. Runs 709-6b, 709-6c, and 709-7, located in the Newfoundland Basin, exhibited backscattering strengths that were clustered around -21 dB. These backscattering strengths were mostly frequency independent, except for Run 709-7, which exhibited a decrease of approximately 4 dB in backscattering strength level between 250 and 600 Hz. Runs 709-2, 709-3, 709-4, 709-5a, and 709-5b, located in the Gloria Drift and the southern end of the Labrador Basin, exhibited backscattering strengths that were clustered around -26 dB, with a slight increase with frequency of approximately 2 dB between 250 and 600 Hz.

Considering the frequency dependence of the Cruise 710 data at 32° grazing angle (Fig. 14), there appeared to be four distinct backscattering strength levels around -24, -30, -33, and -36 dB. The backscattering strengths generally decreased with increasing frequency, although

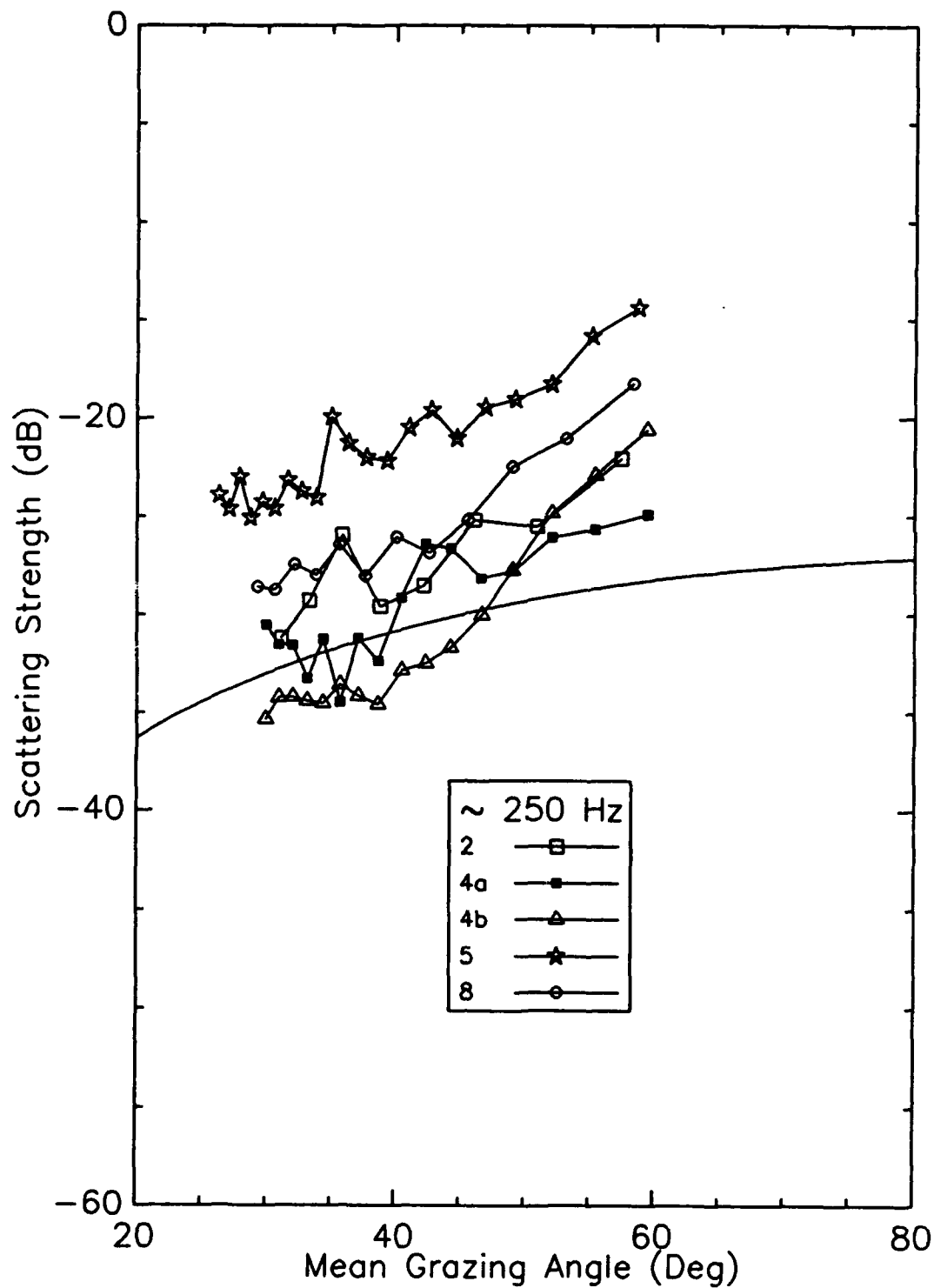


Fig. 9 - Grazing angle dependence of bottom backscattering strengths at 250 Hz for all Cruise 710 ship-based sites. The smooth solid line is the Mackenzie curve.

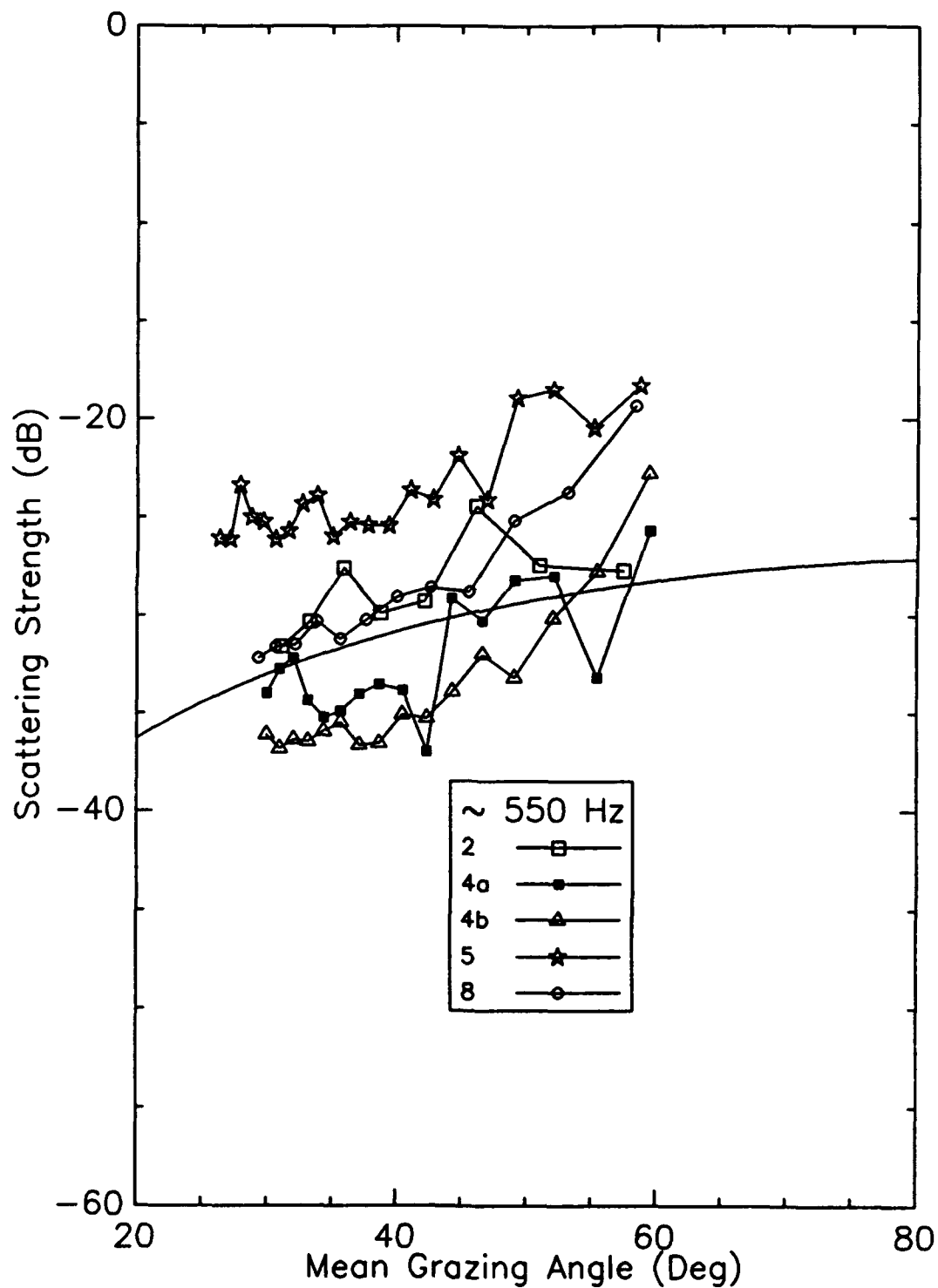


Fig. 10 - Grazing angle dependence of bottom backscattering strengths at 550 Hz for all Cruise 710 ship-based sites. The smooth solid line is the Mackenzie curve.

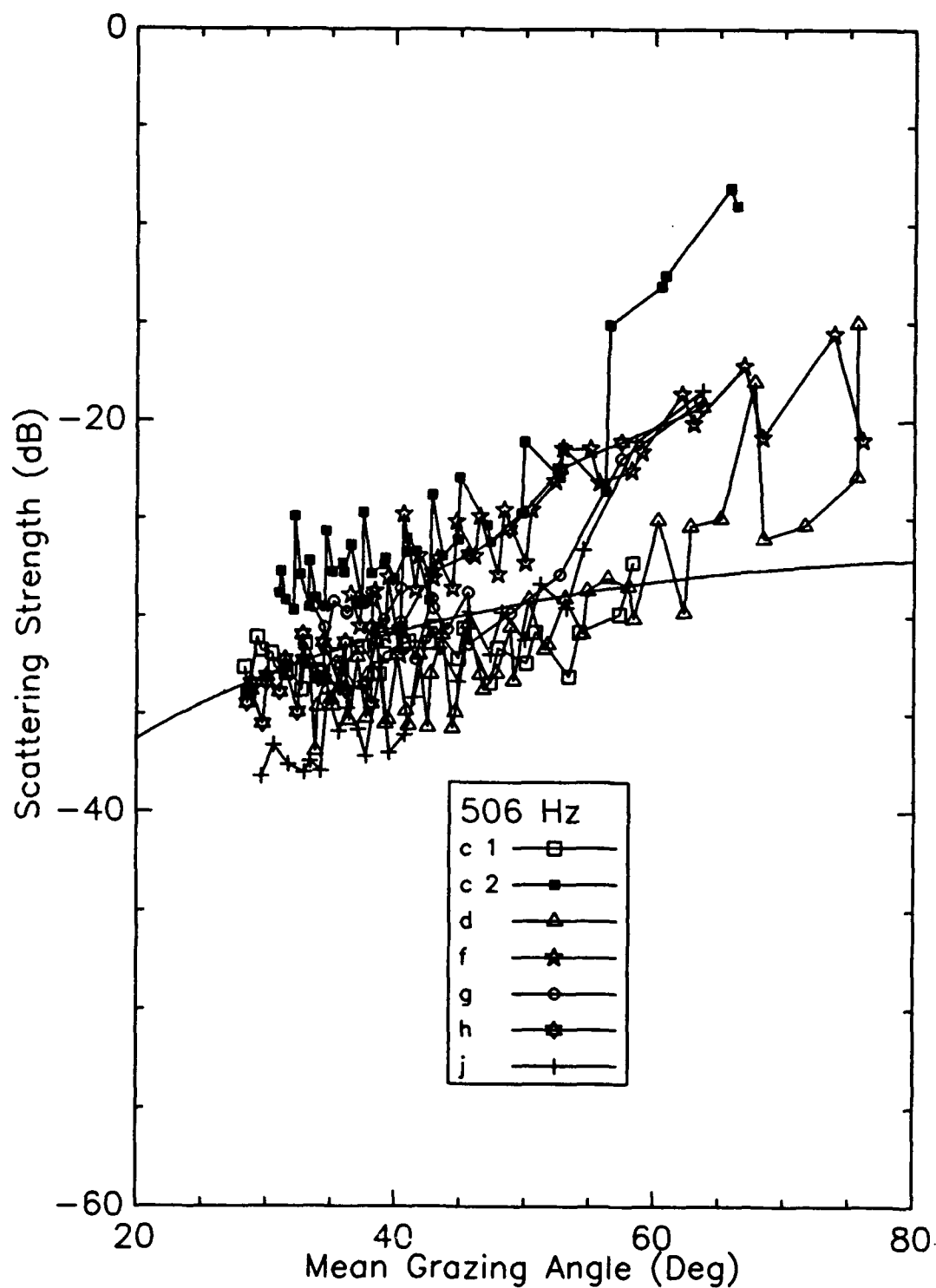


Fig. 11 - Grazing angle dependence of bottom backscattering strengths at 506 Hz for all Cruise 709 and 710 airborne sites. The smooth solid line is the Mackenzie curve.

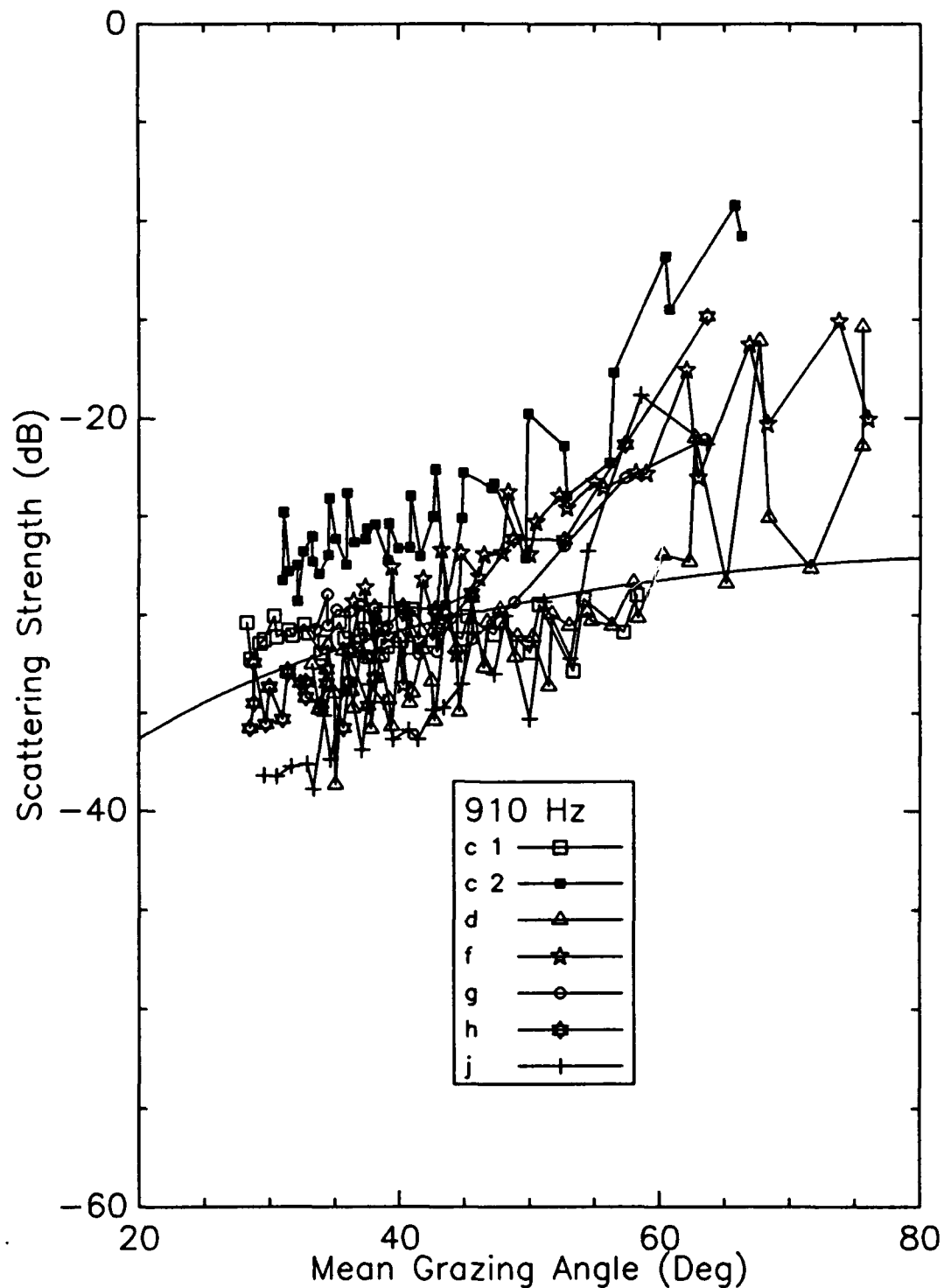


Fig. 12 - Grazing angle dependence of bottom backscattering strengths at 910 Hz for all Cruise 709 and 710 airborne sites. The smooth solid line is the Mackenzie curve.

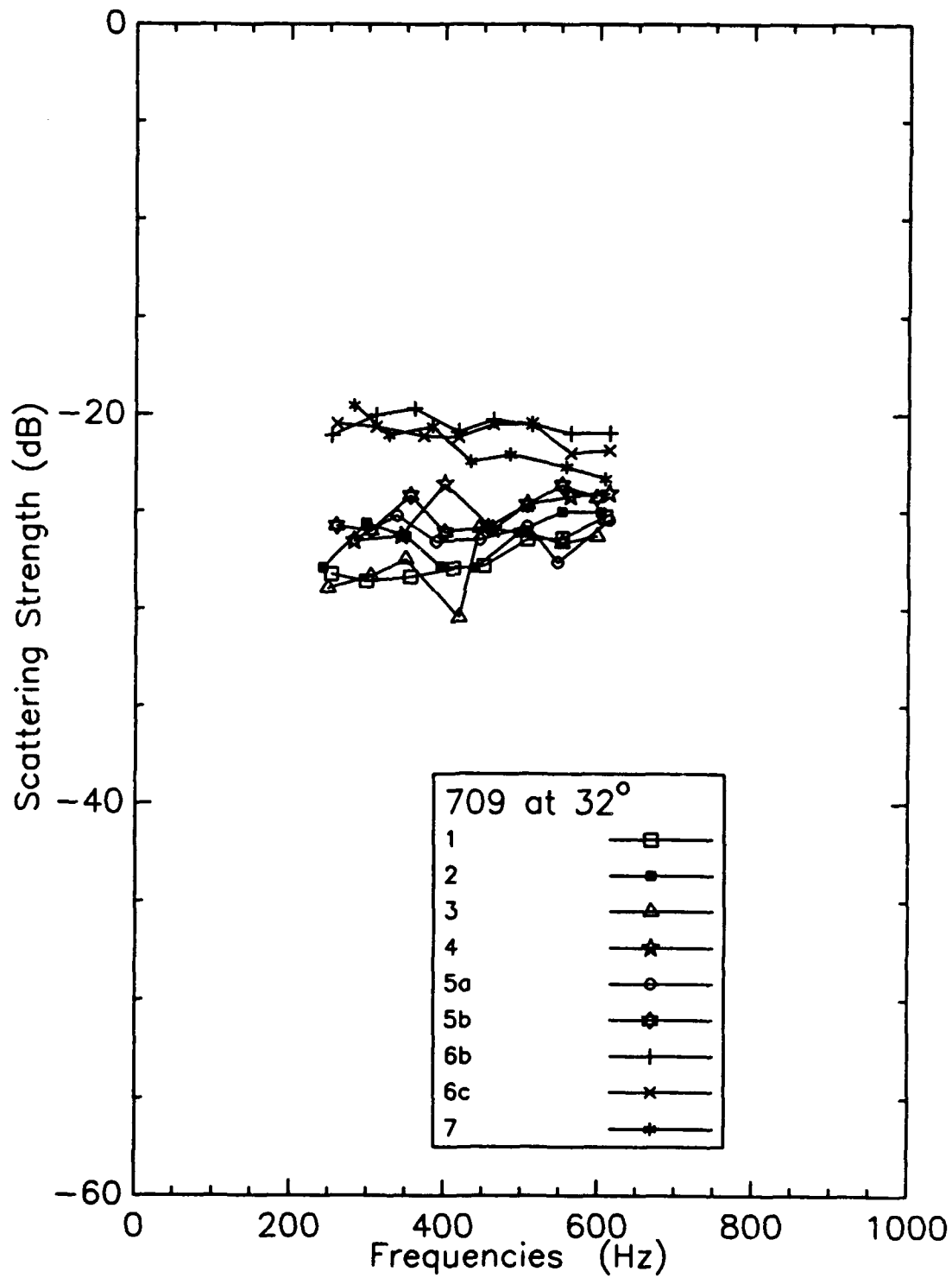


Fig. 13 - Frequency dependence of bottom backscattering strengths at 32° grazing angle for all Cruise 709 ship-based sites

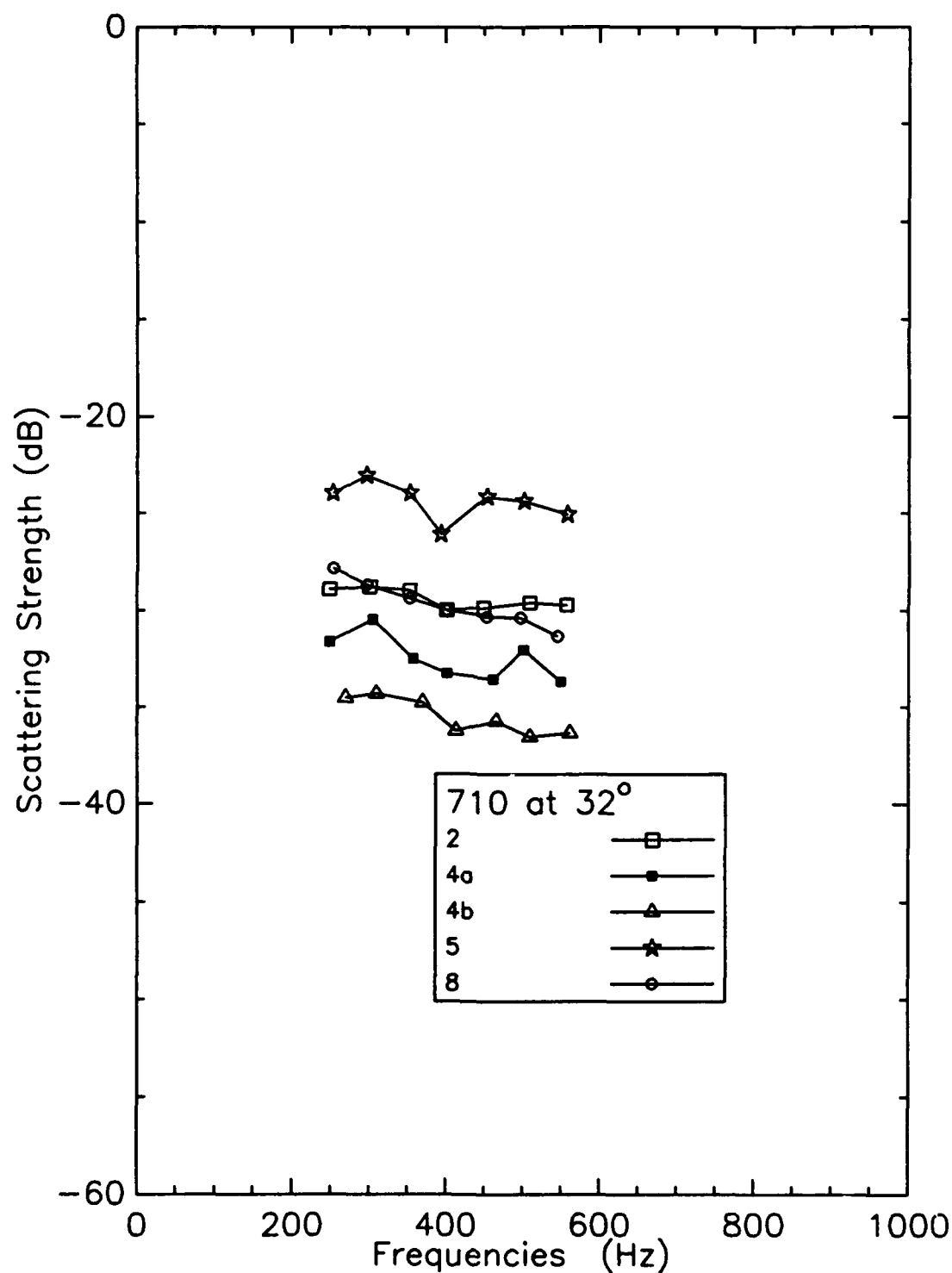


Fig. 14 - Frequency dependence of bottom backscattering strengths at 32° grazing angle for all Cruise 710 ship-based sites

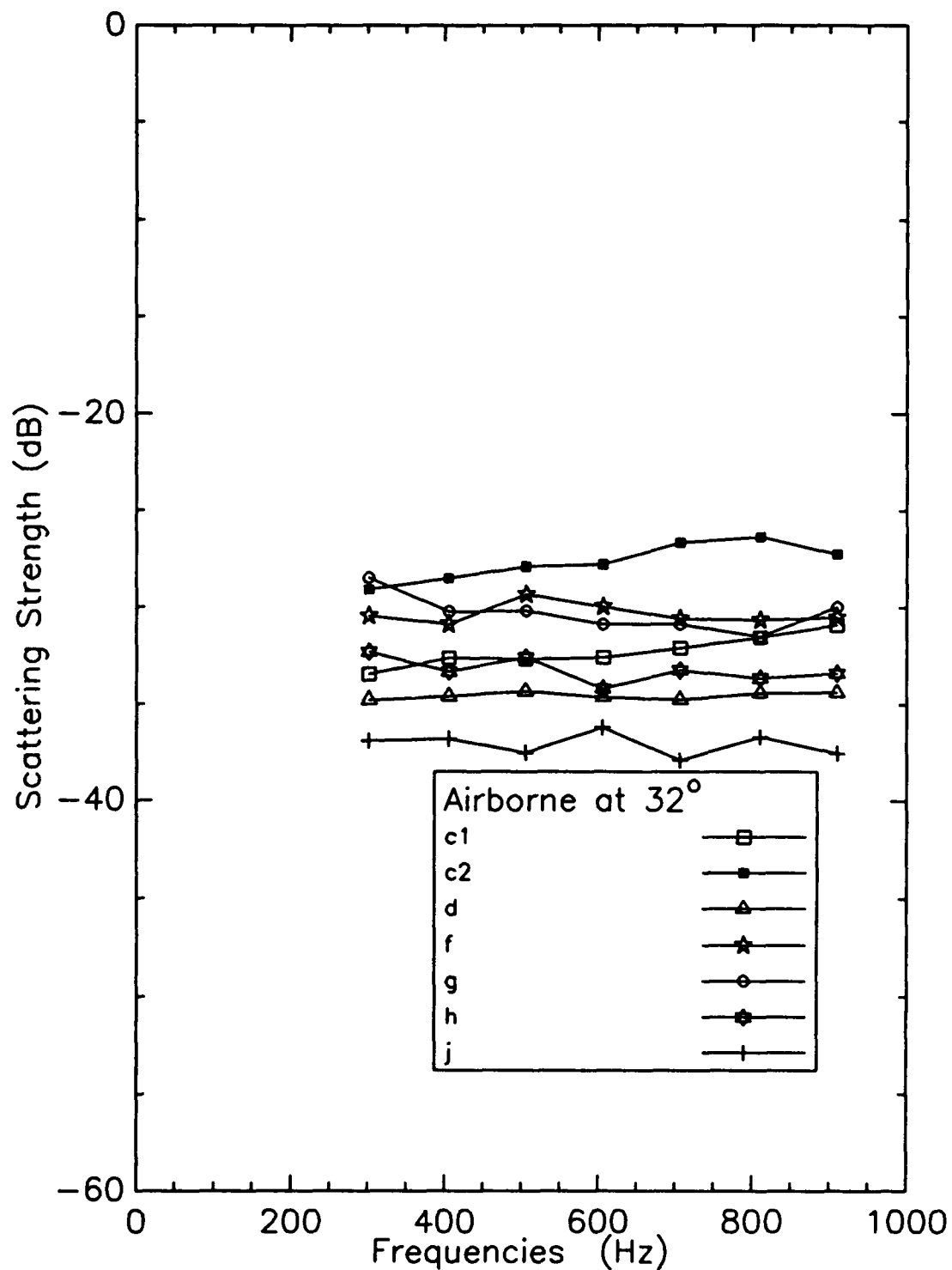


Fig. 15 - Frequency dependence of bottom backscattering strengths at 32° grazing angle for all Cruise 709 and 710 airborne sites

the full range of frequency dependence was less than 3 dB. Run 710-5 showed a noticeable 2 dB dip in backscattering strength around 400 Hz. All the Cruise 710 sites were on the continental rise south of Nova Scotia.

Figure 15 shows the frequency dependence of the Cruise 709 and 710 airborne data at 32° grazing angle. All these flights occurred over areas broadly labeled as regions of turbidite deposition. The backscattering strengths for the Flight c1 site, located in the Gloria Drift, exhibited a slight increase with frequency of approximately 3 dB between 300 and 900 Hz, with a level of -29 dB near 300 Hz. Backscattering strengths for the Flight c2 site, located approximately 19 km south of the Flight c1 site, exhibited similar frequency dependence, but with values about 4 dB higher than for the Flight c1 site. Backscattering strengths for the Flight d, f, h, and j sites were essentially flat across frequency, with average levels varying from -30 to -37 dB. Backscattering strengths for the Flight g site showed a slight decrease with frequency of approximately 3 dB between 300 and 900 Hz, with a level of -28 dB near 300 Hz.

Comparisons with Archival Results

The bottom backscattering strength data were examined to determine if there was a correlation with the Damuth echo character province types [11], which are empirical classifications of the ocean bottom based on the echo character of 3.5 kHz echograms. Table 1 details the Damuth province types of each of the experiment runs. Overall no consistent correlation with the Damuth province types was found. For example, Runs 709-1, 709-3, 710-4a, 710-4b, 710-8, and Flights c2, g, and h all have Damuth province type IA, yet the backscattering strengths at these sites varied over a range of approximately 8 dB and exhibited different frequency dependencies. Even though some runs were near the Damuth province boundaries, which are only roughly accurate, others were not ambiguous and still presented inconsistent types.

Bottom backscattering strengths at 32° grazing angle were also compared with the results of Robison [12] at corresponding locations. Comparisons were made with Robison's results at a fixed grazing angle of 35° in the octave band between 200 and 400 Hz. The results are tabulated in Table 2.

The closest geographic comparison was between Run 710-5 and Robison station 40, with a separation of 7.2 km. The backscattering strengths here were in excellent agreement, differing by only 0.8 dB. There was also good agreement in the Newfoundland Basin area (Runs 709-6b, 709-6c, and 709-7 vs Robison station 102) even though the separations were on the order of 70 km. Backscattering strengths for the various sites on the continental rise were in qualitative agreement, exhibiting a site-to-site variability of approximately 6 dB. The backscattering strength measured for Flight g on the continental slope (-30 dB) was about 5 dB lower than the value of -25.3 dB for Robison station 38. The backscattering strength measured for Flight c1 in the Labrador Basin (-33 dB) was about 6 dB higher than the value of -38.8 dB for Robison station 121. Overall the measured bottom backscattering strengths and the Robison values were within approximately 6 dB of each other.

Table 2 – Comparison of Bottom Backscattering Strengths Measured by NRL with Results of Robison

Robison Station	Latitude	Longitude	SS (dB)	Physiographic Province Type	Damuth Type	NRL Run	SS (dB)	Separation (km)
38	42° 47' N	61° 03' W	-25.3	Continental Slope	IA	g	-30	22.9
39	41° 58' N	60° 58' W	-26.6	Continental Rise	IA	710-5	-24	14.3
40	41° 51.5' N	60° 51' W	-24.8	Continental Rise	V			7.2
41	41° 45' N	60° 42' W	-27.9	Continental Rise	V			20.4
104	50° 26' N	44° 45' W	-33.2	Continental Rise	General	709-4	-21	91.9
121	54° 40' N	43° 40' W	-38.8	Labrador Basin	V	c1	-33	87.8
102	44° 00' N	44° 28' W	-22.0	Newfoundland Basin	IIA	709-6b	-21	73.8
						709-6c	-21	73.8
						709-7	-21	70.3

COMPARISON OF EXPERIMENTAL TECHNIQUES

Comparison Between Ship-Based and Airborne Techniques

It is of interest to compare the results obtained from the ship-based technique using the towed line array receiver with those from the airborne technique using the omnidirectional sonobuoys. In general one could expect the ship-based technique to give more accurate results, since the towed array beampattern can discriminate against fathometerlike returns and since the detonation of the SUS beneath the receiver is more consistent. However, since the airborne SUS and sonobuoys are readily deployable, the airborne technique is more suitable for large-area surveys. Moreover, the airborne technique remains more strictly at a single site (assuming the drift rate is small). Thus, one would like to verify that the airborne technique gives results comparable to those of the ship-based technique.

To facilitate this comparison, SUS tests of both types were conducted at sites within approximately 1.5 km of each other. Comparisons from three locations are presented in Figs. 16 to 21. (See Fig. 1 for geographic locations.) These plots present results at 300 and 500 Hz.

In all cases the variability between the ship-based and airborne results was approximately 5 dB. Moreover, there was no significant difference between the behavior at grazing angles above 40°, suggesting that beampattern suppression of fathometerlike returns did not have much effect.

Merging vs Averaging in Scattering Strength Computations

The standard data analysis technique was to merge the different SUS shots in a run by taking a linear average of the reverberation levels and then computing a single set of backscattering strengths using an average value for the source-receiver separation. One could, however, compute the backscattering strengths for each shot individually using the individual source-receiver separations and then average the backscattering strengths directly. In principle, the results can be different since the propagation is not linear in the source-receiver separation.

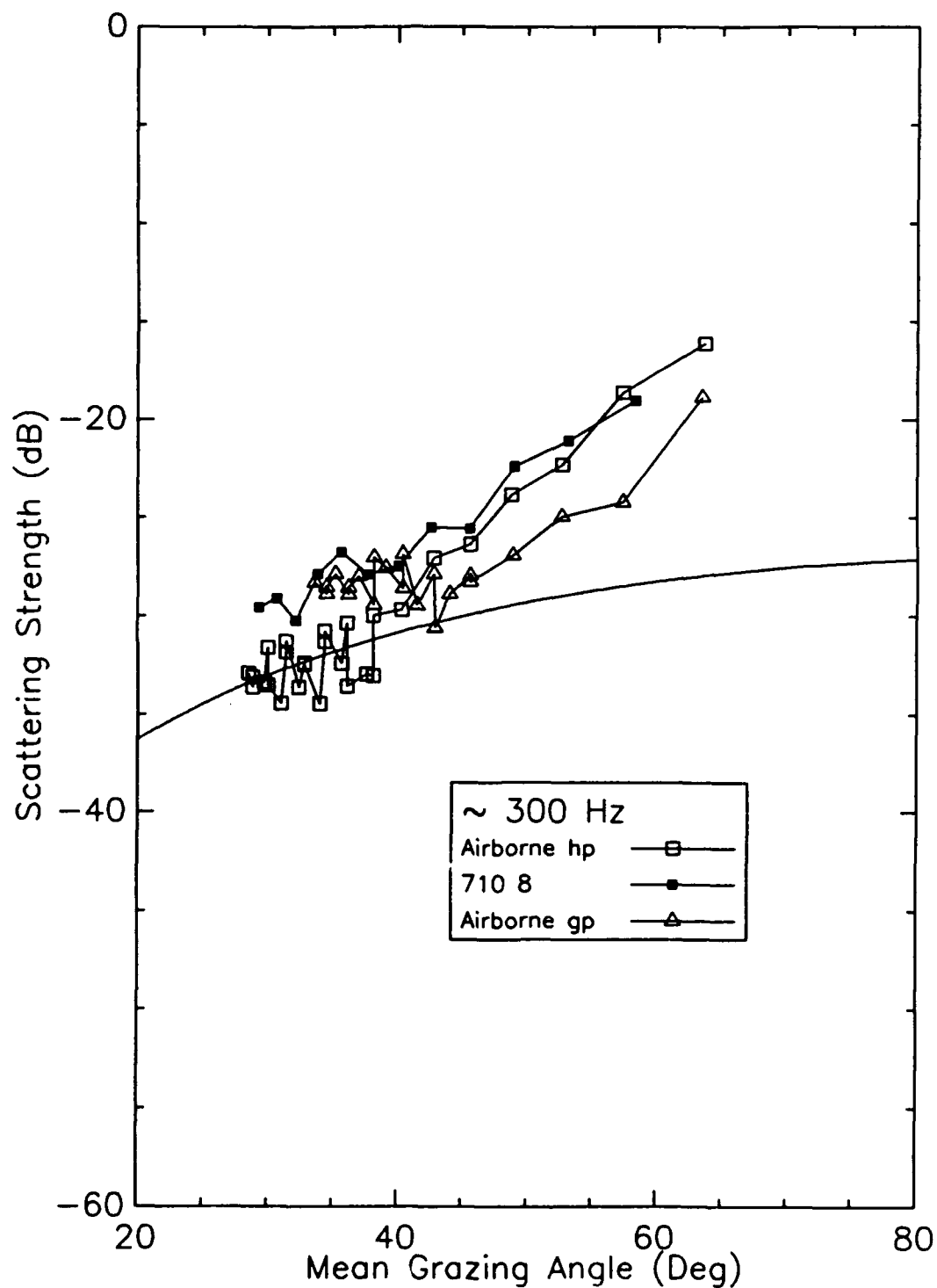


Fig. 16 - Same-site comparison of selected ship-based and airborne bottom backscattering strength measurements at 300 Hz. The results shown are for Run 710-8, 710 Flight g, and 710 Flight h. The smooth solid line is the Mackenzie curve.

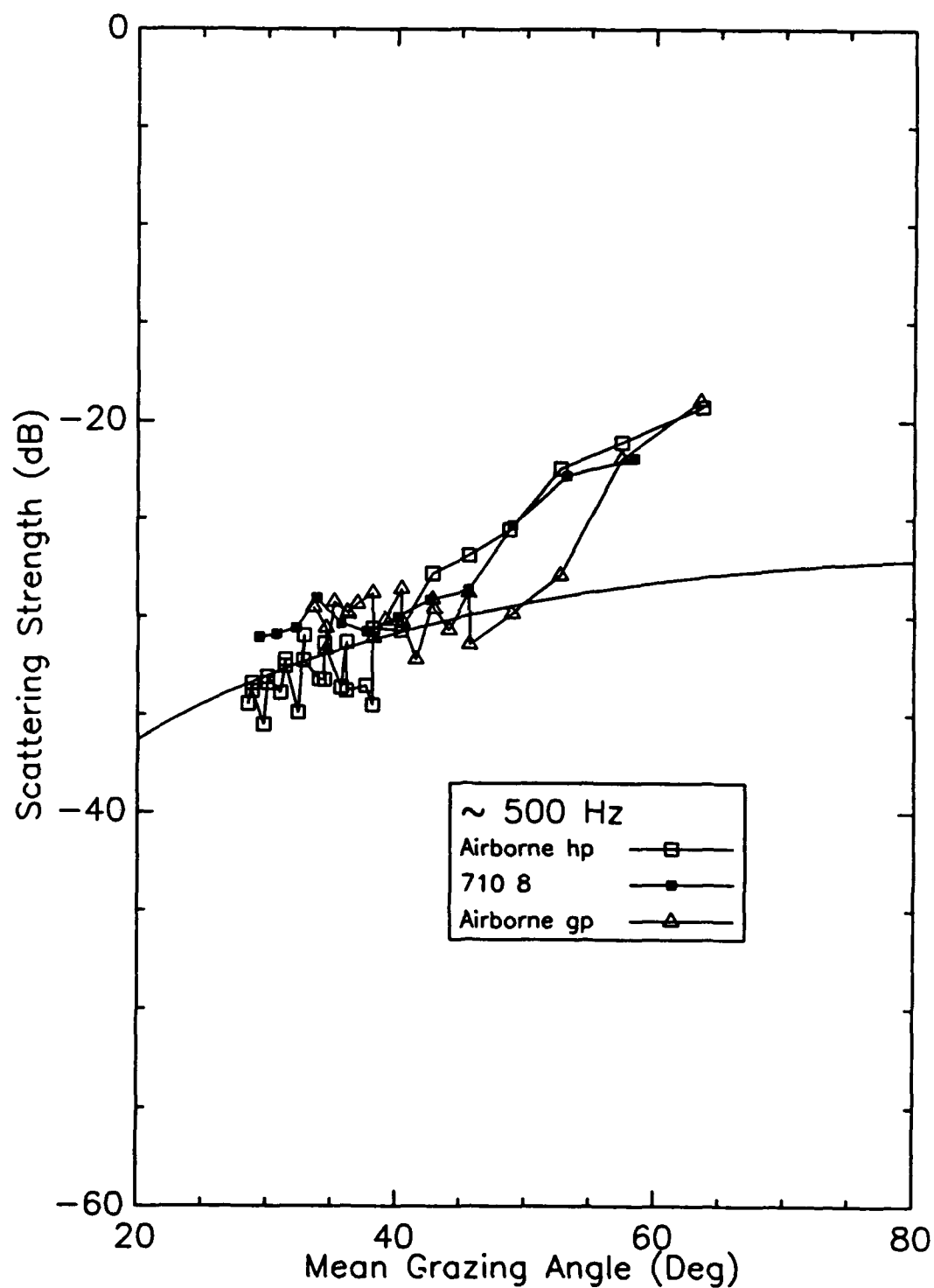


Fig. 17 - Same-site comparison of selected ship-based and airborne bottom backscattering strength measurements at 500 Hz. The results shown are for Run 710-8, 710 Flight g, and 710 Flight h. The smooth solid line is the Mackenzie curve.

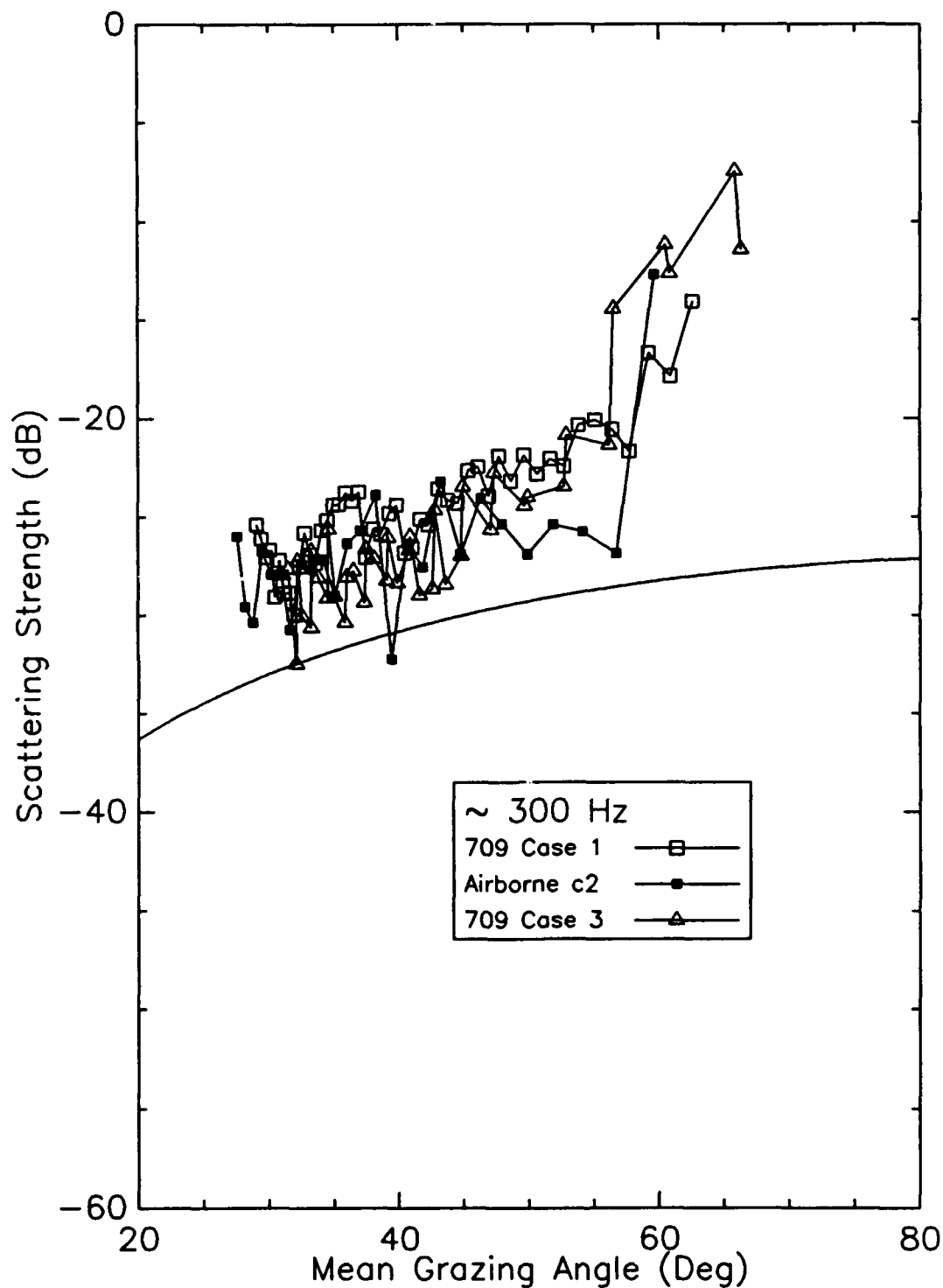


Fig. 18 - Same-site comparison of selected ship-based and airborne bottom backscattering strength measurements at 300 Hz. The results shown are for Run 709-1, Run 709-3, and 709 Flight c2. The smooth solid line is the Mackenzie curve.

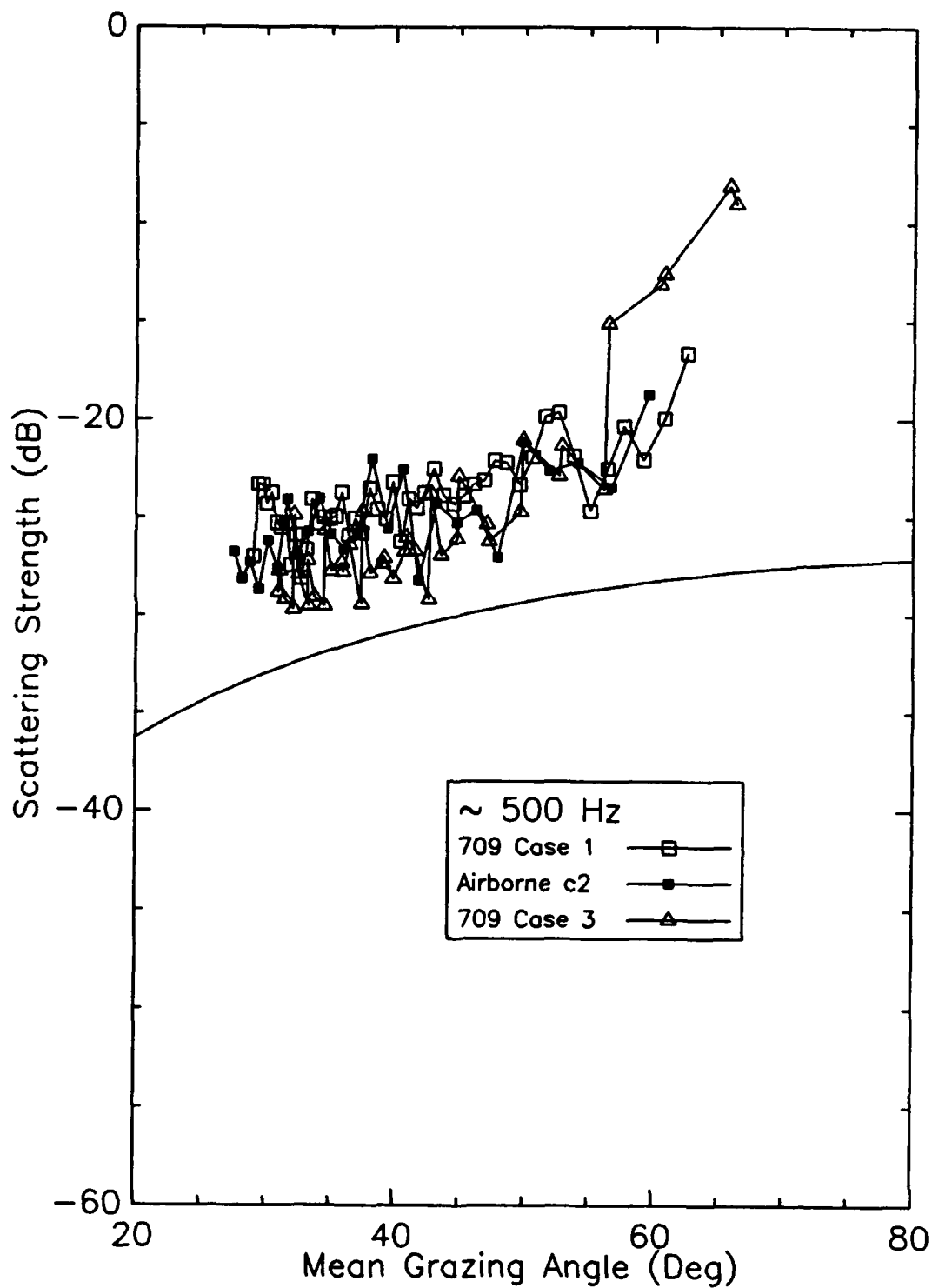


Fig. 19 - Same-site comparison of selected ship-based and airborne bottom backscattering strength measurements at 500 Hz. The results shown are for Run 709-1, Run 709-3, and 709 Flight c2. The smooth solid line is the Mackenzie curve.

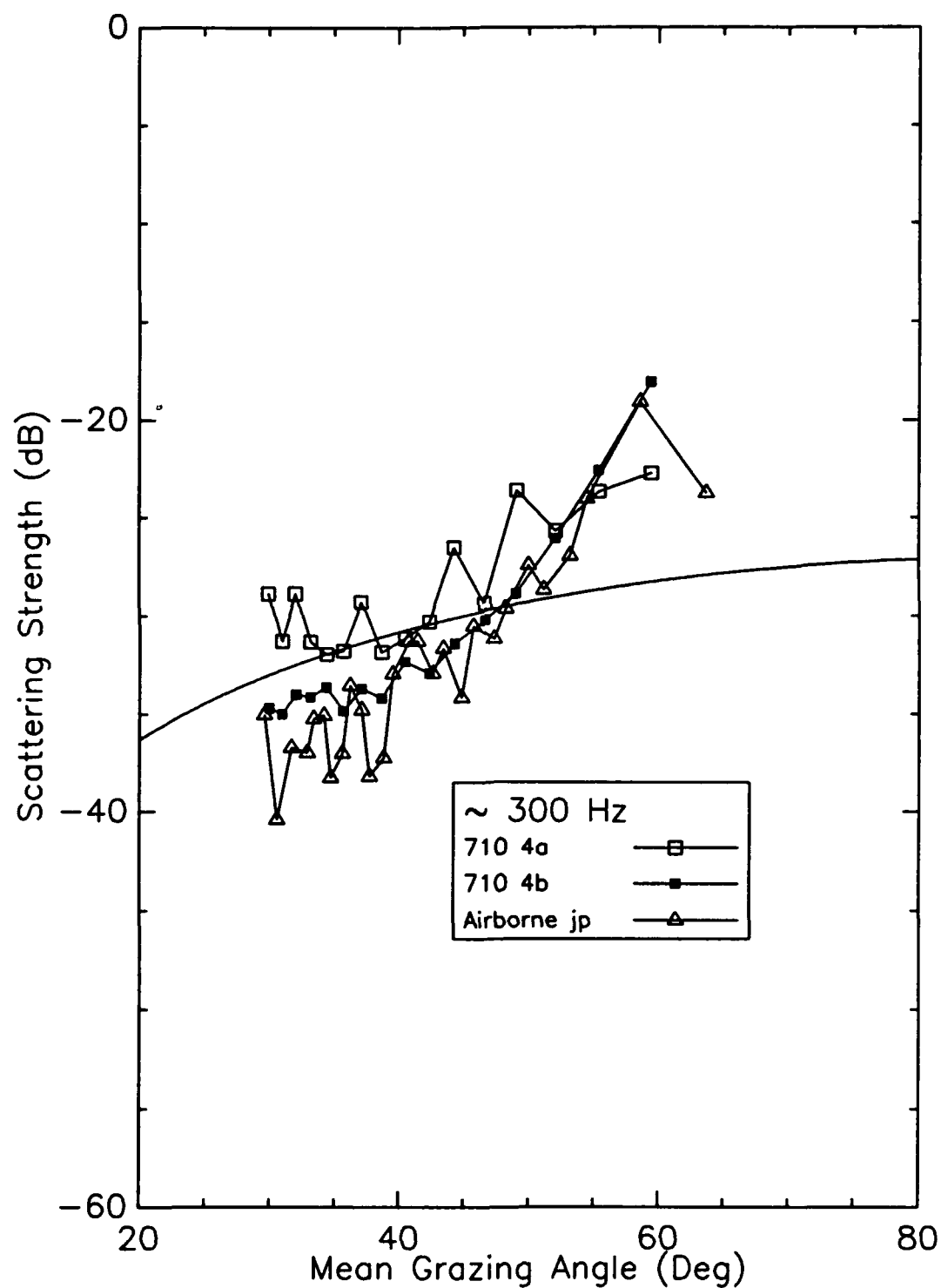


Fig. 20 - Same-site comparison of selected ship-based and airborne bottom backscattering strength measurements at 300 Hz. The results shown are for Run 710-4a, Run 710-4b, and 710 Flight j. The smooth solid line is the Mackenzie curve.

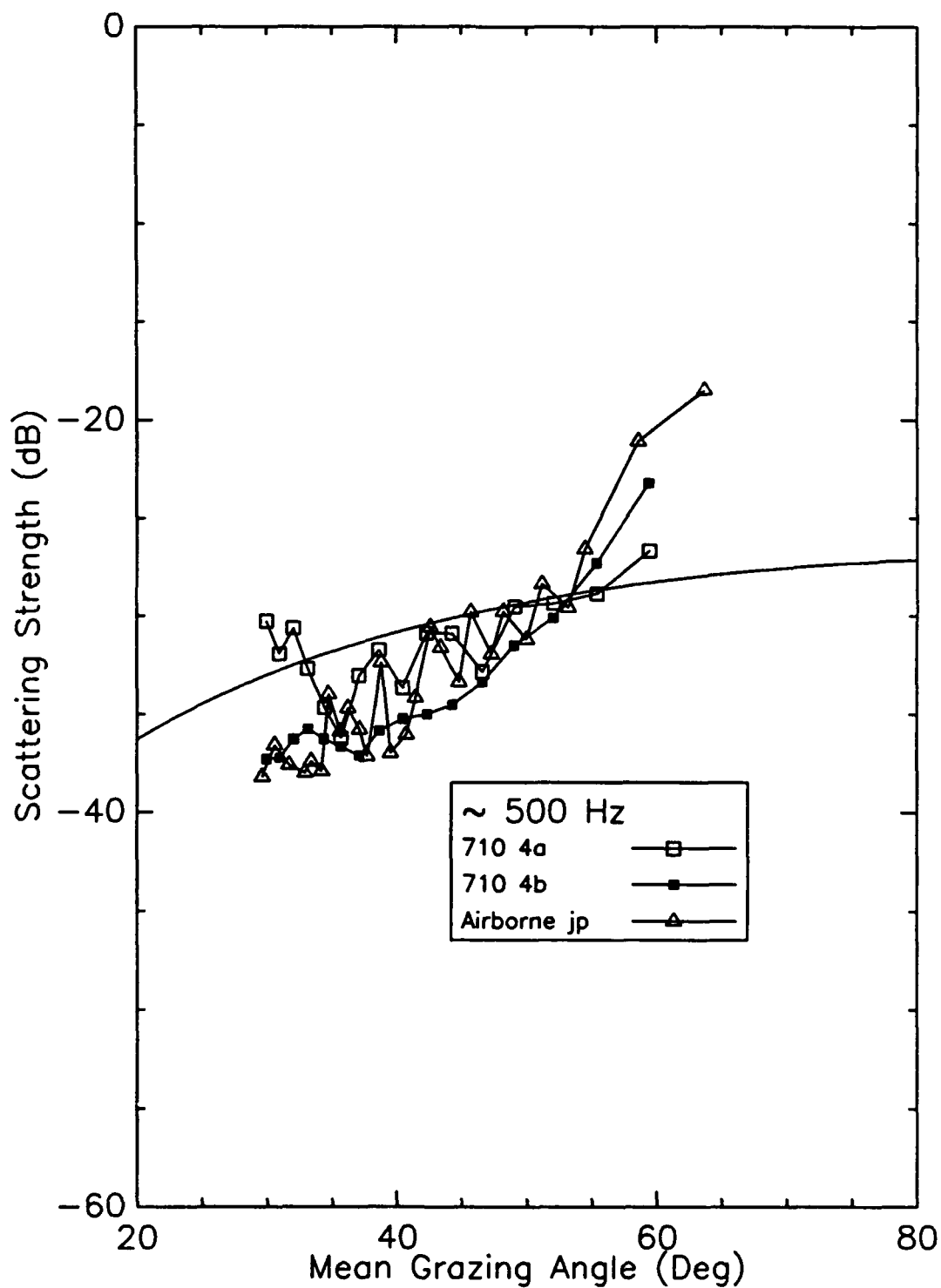


Fig. 21 - Same-site comparison of selected ship-based and airborne bottom backscattering strength measurements at 500 Hz. The results shown are for Run 710-4a, Run 710-4b, and 710 Flight j. The smooth solid line is the Mackenzie curve.

Figures 22 to 24 present results of this comparison for backscattering strengths at the Flight d site. The dashed line represents the results obtained by merging the reverberation from individual shots and then computing a single set of backscattering strengths. The dotted line represents the average of the individual SUS shot backscattering strengths in dB. Each average is over 33 points and is plotted at the average grazing angle for this ensemble. Error bars for one sample standard deviation are also shown. One can see that the merging technique generally gave results within the statistical spread of the ensemble of individual shots, indicating that the standard merging technique is adequate relative to the overall accuracy of the data.

SUMMARY AND CONCLUSIONS

This report has discussed measurements of ocean surface and bottom backscattering strengths that were made by NRL in July and August 1990 in the northwestern Atlantic Ocean. The experiment was carried out during two cruises, known as Cruise 709-90 and Cruise 710-90. The first of these was part of a joint exercise with the Canadian Defence Research Establishment Atlantic (DREA). This cruise took place primarily in two areas in the northwestern Atlantic Ocean, one approximately 1000 km northeast of the Grand Banks and the other approximately 450 km southeast of the Grand Banks. The second cruise took place approximately 250 km south of Nova Scotia. Both cruises were conducted using the USNS *Lynch* research vessel, which deployed the NRL towed horizontal line array receiver. They were supported by a Navy P-3 aircraft, which deployed omnidirectional sonobuoy receivers to make comparison measurements at the ship-based experimental sites as well as other sites.

The primary scientific objective of the experiment was to characterize the dependence of ocean surface and bottom backscattering strengths on environmental parameters such as grazing angle, frequency, wind speed (for the surface), and geophysical parameters (for the bottom). These dependencies are important for understanding the character of long-range reverberation for active sonar systems. The range of sampled environmental parameters included wind speeds between 1.0 and 12.3 m/s and bottom depths between 2215 and 4790 m. Bottom grazing angles down to 30° were achieved.

The experiment used ship and air deployed explosive charges to provide ensonification of the ocean surface and bottom over a broad range of low frequencies up to 1 kHz. Two experimental techniques were used. In the ship-based technique, the explosive SUS (Signals, Underwater Sound) charges were detonated approximately directly beneath the towed line array receiver in a quasi-monostatic geometry. These ship-based backscattering strength measurements were analyzed at selected frequencies between 250 and 600 Hz. In the airborne technique, a suite of three sonobuoys with different attenuations was deployed at a single location to measure the full dynamic range of the reverberation. The aircraft then flew a "90-270" pattern (shaped like a barbell or figure eight) and dropped SUS charges at the crossover point above the sonobuoys, again achieving a quasi-monostatic geometry. The airborne backscattering strength measurements were analyzed at selected frequencies between 250 and 1000 Hz.

The ocean surface and bottom backscattering strengths were extracted from the measurements via the sonar equation. This was accomplished using the expected source level and calculating the transmission loss and backscattering area.

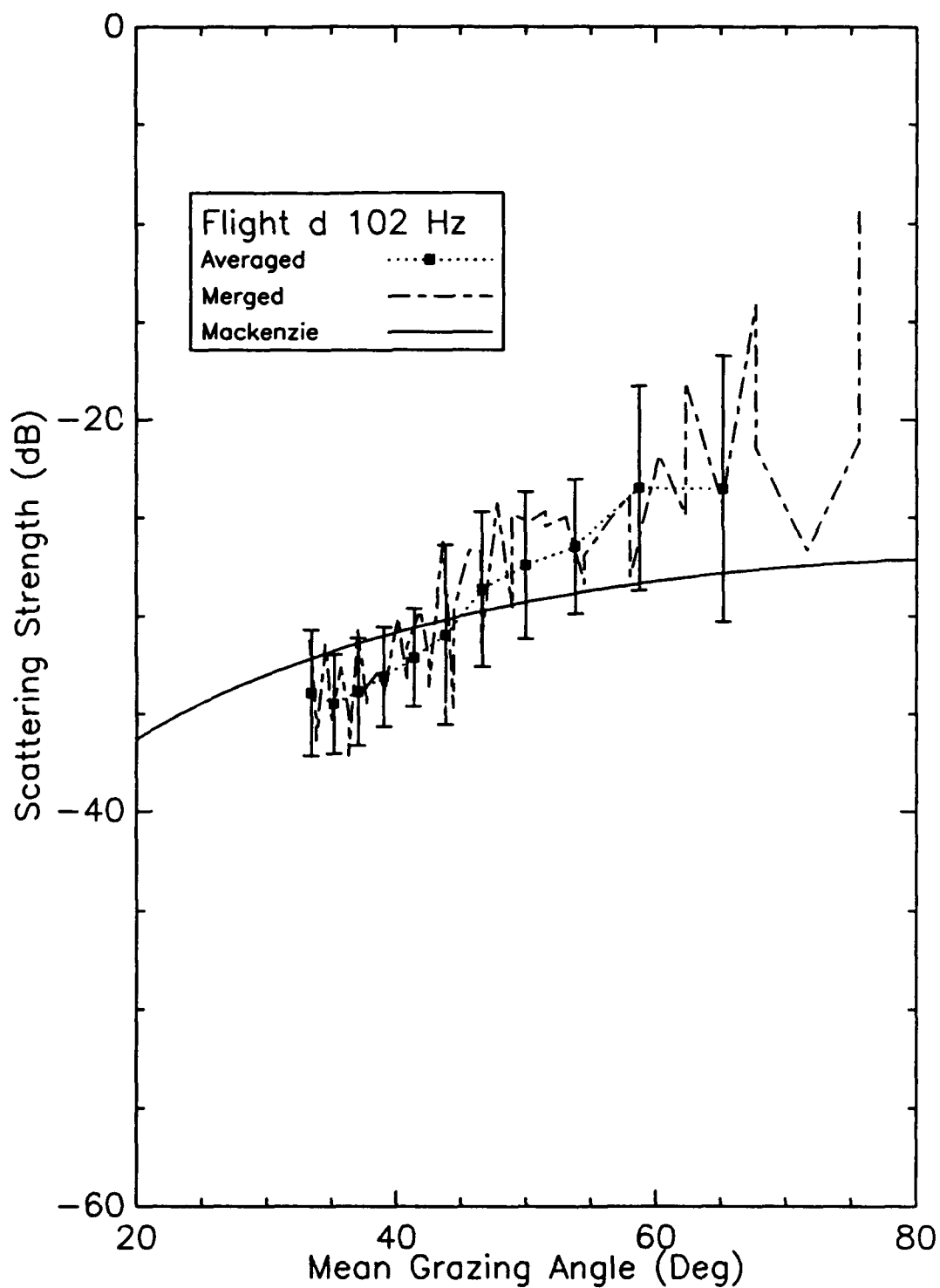


Fig. 22 - Merged vs averaged backscattering strengths for 709 Flight d at 102 Hz. The smooth solid line is the Mackenzie curve.

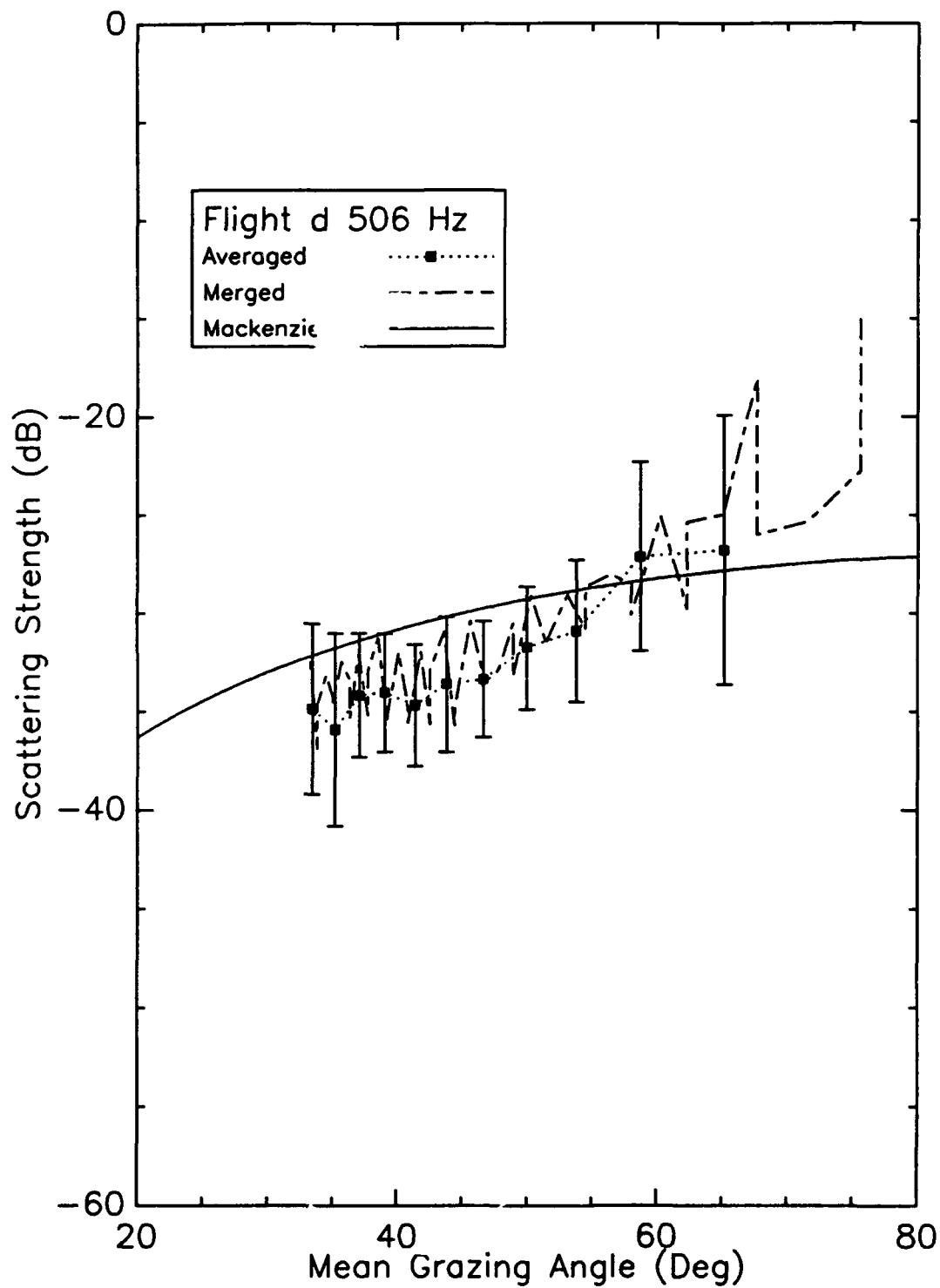


Fig. 23 - Merged vs averaged backscattering strengths for 709 Flight d at 502 Hz. The smooth solid line is the Mackenzie curve.

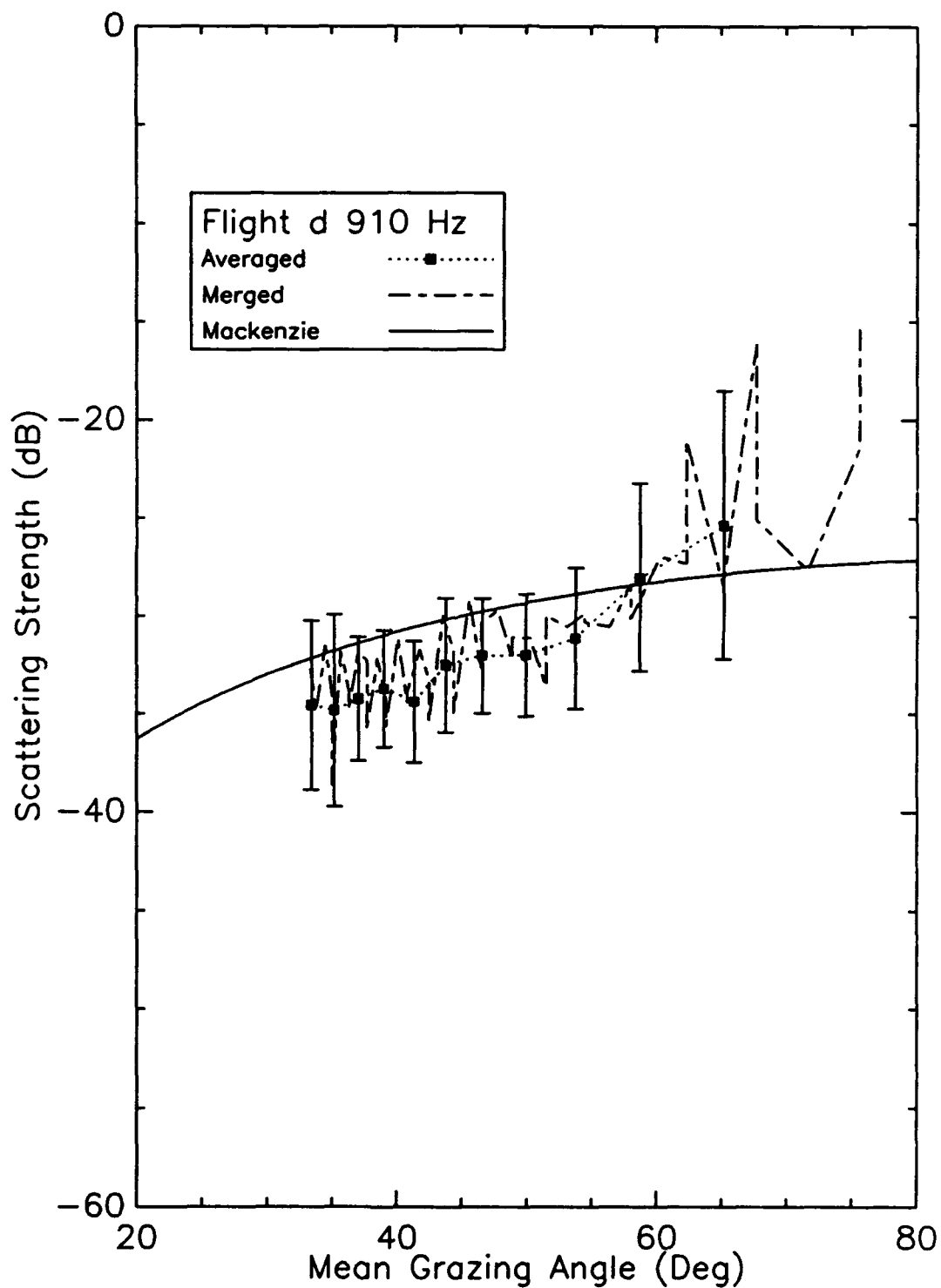


Fig. 24 - Merged vs averaged backscattering strengths for 709 Flight d at 910 Hz. The smooth solid line is the Mackenzie curve.

Surface Backscattering Strengths

Overall the surface backscatter results agreed reasonably well with the Ogden-Erskine curves [4], matching the predicted dependence on wind speed, grazing angle, and frequency.

At two sites located northeast of the Grand Banks the surface backscattering strengths appeared to be dominated by volume backscattering caused by fish, as evidenced by a lack of dependence of the backscattering strengths on grazing angle.

Bottom Backscattering Strengths

The bottom backscattering strengths were observed to have considerable variation in level between different sites. For example, in the frequency range 200 to 400 Hz at 32° grazing angle, the backscattering strengths exhibited a 17 dB variation between -20 and -37 dB.

As a function of grazing angle, most of the backscattering strength curves approximately paralleled the Mackenzie curve for grazing angles between 30° and 50°. This was true for several sites in the Gloria Drift and the southern end of the Labrador Basin, with levels approximately 6 dB above the Mackenzie curve. It was also true for several sites on the continental rise south of Nova Scotia, with levels variable from 2 dB above the Mackenzie curve to 4 dB below it. However, a few sites in the Newfoundland Basin and on the continental rise south of Nova Scotia exhibited backscattering strength curves flatter than the Mackenzie curve below 40° grazing angle, with levels ranging from 12 to 14 dB above the Mackenzie curve at 30° grazing angle to 4 dB below it.

A moderate frequency dependence of approximately 3 dB was observed in the measured bottom backscattering strengths between 250 and 1000 Hz. At sites in the Gloria Drift and the southern end of the Labrador Basin the backscattering strengths were observed to increase with increasing frequency. At sites in the Newfoundland Basin and some sites on the continental rise south of Nova Scotia the backscattering strengths decreased with increasing frequency. At other sites on the continental rise south of Nova Scotia the backscattering strengths were approximately flat across frequency.

Comparisons of the bottom backscattering strengths with the Damuth 3.5 kHz echo character province types yielded no consistent correlations.

Comparisons of measured bottom backscattering strengths with the results of Robison [12] yielded general agreement within 6 dB. The best agreement was for Robison station 40 on the continental rise south of Nova Scotia (within 0.8 dB), although in general this slope region exhibited a variability of approximately 6 dB. Good agreement was also obtained at sites in the Newfoundland Basin.

Comparison of Experimental Techniques

The ship-based technique, using a towed horizontal line array receiver, and the airborne technique, using omnidirectional sonobuoy receivers, yielded comparable backscattering strength results that were within approximately 5 dB of each other.

The standard technique of merging the reverberation levels from several SUS shots and then computing a single set of backscattering strengths (using an average source-receiver separation) was shown to be adequately equivalent to the computation of backscattering strengths for each of the shots separately using individual source-receiver separations and then taking the average of the individual shot backscattering strengths.

ACKNOWLEDGMENTS

This research was supported by the Office of Naval Research, Code 234. One of the authors (F. Erskine) was test scientist for Cruise 709-90. The authors gratefully acknowledge the effort of Jonathan Berkson, the test scientist for Cruise 710-90, towards the planning and conduct of that exercise. The authors express thanks to Frederick Facemire for his work in the initial stages of the processing of the airborne data, and to Brenda Vest (Planning Systems, Inc.) and Brian Walsh for their help in processing the backscattering strength data. The authors also express thanks to Peter Ogden for useful comments and suggestions, and to David Fromm for assistance in document preparation.

REFERENCES

1. R. P. Chapman and J. H. Harris, "Surface Backscattering Strengths Measured with Explosive Sound Sources," *J. Acoust. Soc. Am.* **34** (10), 1592-1597 (1962).
2. R. P. Chapman and H. D. Scott, "Surface Backscattering Strengths Measured over an Extended Range of Frequencies and Grazing Angles," *J. Acoust. Soc. Am.* **36**, 1735-1737 (1964).
3. Eric I. Thorsos, "Acoustic scattering from a 'Pierson-Moskowitz' sea surface," *J. Acoust. Soc. Am.* **88**, 335-349 (1990).
4. Peter M. Ogden and Fred T. Erskine, "An Empirical Prediction Algorithm for Low-Frequency Acoustic Surface Scattering Strengths," NRL Formal Report, NRL/FR/5160-92-9377, Naval Research Laboratory, Washington, D.C. (1992).
5. K. V. Mackenzie, "Bottom Reverberation for 530- and 1030-cps Sound in Deep Water," *J. Acoust. Soc. Am.* **33**, 1498-1504 (1961).
6. E. Kim, "Direct Path Software User's Guide," NRL internal document (unpublished), 1992.
7. R. Pitre, P. Davis, M. A. Childers, S. M. Brylow, and F. T. Erskine, "A ray trace program for calculating direct path surface and bottom backscatter propagation loss and grazing angles (U)," NRL Memo 5160-619 (1986).
8. Robert J. Urick, *Principles of Underwater Sound*, 3rd ed., (McGraw-Hill, New York, 1983).
9. R. J. Urick, "Handy Curves for Finding the Source Level of an Explosive Charge Fired at a Depth in the Sea," *J. Acoust. Soc. Am.* **49**, 935-936 (1971).
10. P. M. Ogden and F. T. Erskine, "Surface backscattering measurements using broadband SUS charges in the Critical Sea Test experiments," *J. Acoust. Soc. Am.* (submitted, 1993).

11. E. P. Laine, J. E. Damuth, and Robert Jacobi, "Surficial sedimentary processes revealed by echo-character mapping in the western North Atlantic Ocean," in *The Geology of North America, Volume M, The Western North Atlantic Region*, P. R. Vogt and B. E. Tucholke, eds., The Geological Society of America, 1986.
12. A. E. Robison, "Bottom Reverberation in the North Atlantic," DREA Technical Memorandum 75/B, Defence Research Establishment Atlantic, Dartmouth, N. S., Canada (1975).

Appendix A

CALIBRATION FOR THE NRL TOWED LINE ARRAY PROCESSING SYSTEM

THE NRL TOWED LINE ARRAY

The NRL towed line array [A1] comprises 64 hydrophones grouped into four nested subarrays with design frequencies of 75, 150, 300, and 600 Hz (Table A1). The hydrophones used in processing the Cruise 709-90 and Cruise 710-90 ship-based surface and bottom backscatter experiment data were part of the 600 Hz subarray (channels 42 through 64) on the forward end of the array.

Table A1 – NRL Towed Line Array Specifications

Number of Hydrophones	Hydrophone Spacing (m)	Aperture Length (m)	Design Frequency (Hz)
30	10.00	290.0	75
21	5.00	100.0	150
27	2.50	65.0	300
23	1.25	27.5	600

Figure A1 diagrams the typical electronic configuration during data collection.

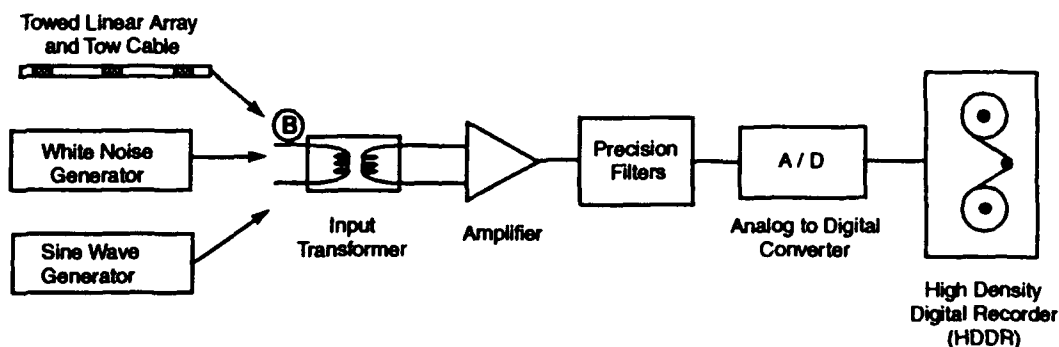


Fig. A1 – Typical electronic configuration during data collection

COMPONENT ANALYSIS

The Teledyne Exploration Model T-2 Hydrophone Specifications document lists the hydrophone sensitivity as $-194.4 \text{ dB re } 1\text{V}/\mu\text{Pa}$, as measured by NRL-Orlando.

From Ref. [A2], two transformers are present in the towed array system. Each transformer gives a calibration factor of $-20 \log[\rho]$, where ρ is the transformer turns ratio. The first is a $\sqrt{10} : 1$ step-down transformer located in the array itself. The second is a $1 : 2$ step-up transformer just

before the amplifier (after point B in Fig. A1). The calibration factors are -10.0 and +6.0 dB, respectively, giving a net value of -4.0 dB. Also, Ref. [A2] calculates a line loss of -4.3 dB for the array, tow cable, deck leader, and input transformers. However, in 1985 the electronics were modified by replacing a 5.49k Ω resistor with a 348k Ω resistor, so that the calculated line loss is now negligible (< 0.1 dB).

The nominal value of the amplifier gain is $20 \log[500] = +54.0$ dB.

The Phoenix analog-to-digital (A/D) converter has an input range of ± 10 V, with 15 bits of binary output. The gain is thus $20 \log[(2^{15})/(20.)] = 64.3$ dB.

Postprocessing of the data was accomplished with NRL GENPASS computer program that Fourier transforms the data to the frequency domain and beamforms the data. The GENPASS program gives the following calibration factors: The temporal FFT should be normalized by $10 \log[2N^2]$, where N is the FFT size. For Cruise 709-90 ship-based data with $N = 1024$, this was 63.2 dB. For Cruise 710-90 ship-based data with $N = 512$, this was 57.2 dB. The spatial FFT (beamforming) should be normalized by $10 \log[M^2]$, where M is the number of hydrophones. For $M = 16$, this was 24.1 dB. Temporal and spatial Hamming shading each give a loss of -4.0 dB.

Table A2 lists the calibration values.

Table A2 - Calibration via Component Analysis

Factor	Value (dB)	
	709-90	710-90
Hydrophone Sensitivity	-194.4	-194.4
Transformers	-4.0	-4.0
Amplifier Gain	+54.0	+54.0
A/D Gain	+64.3	+64.3
FFT Size (temporal)	+63.2	+57.2
Hamming Shading (temporal)	-4.0	-4.0
FFT Size (spatial)	+24.1	+24.1
Hamming Shading (spatial)	-4.0	-4.0
TOTAL	-0.8	-6.8

EMPIRICAL WHITE NOISE ANALYSIS

An empirical calibration was performed based on the white noise calibration Run 006 (709-90 Cruise Log No. 1, pp. 32-33). The input at point B in Fig. A1 was measured to be -73.6 dBV/ $\sqrt{\text{Hz}}$ (at the frequency 350 Hz). The white noise calibration data was postprocessed using GENPASS (with $N = 2048$ and Hamming shading in time) to produce a "lines" file containing the complex-valued frequency line spectra for the data. This "lines" file was then run through the program DBCALFILE, written by Bruce Pasewark, to produce an empirical calibration curve based on the ensemble-averaged white noise data. The parameters supplied to this program were an input level (relative to point B) of -73.6 dBV/ $\sqrt{\text{Hz}}$ and an effective hydrophone sensitivity (including the gain from the $\sqrt{10} : 1$ step-down transformer in the array itself) of -204.4 dB re 1V/ μPa . A mathematical fit to the resulting empirical calibration curve was then obtained using the program STAT4RUN, written by Nolan Davis. The parameters of the fit were a constant offset and the

corner frequencies for three high-pass filters, each with a 6 dB/octave rolloff at low frequency. These filters corresponded to the two pre-whitening filters in the system, plus an additional high-pass filter response resulting from the non-ideal transformer used to couple the white noise generator into the system. The nominal pre-whitening component values are listed in Ref. [A3], corresponding to nominal corner frequencies of 234 and 195 Hz. The nominal measured corner frequency for the white noise generator input transformer was 98 Hz. However, the best fit frequencies were 150, 156, and 159 Hz. The best fit offset was -18.5 dB, which corresponded to the asymptotic high frequency calibration value. These parameters gave a very good fit to the empirical calibration curve, whereas the nominal values did not.

The differences in temporal FFT sizes between the white noise calibration run and the data collection runs required an adjustment of $10 \log[(1024^2)/(2048^2)] = -6.0$ dB for the Cruise 709-90 ship-based data, and $10 \log[(512^2)/(2048^2)] = -12.0$ dB for the Cruise 710-90 ship-based data.

Table A3 lists the white noise empirical analysis calibration values. The net calibration value is 3.6 dB lower than the value determined by the component analysis, indicating a possible additional loss in the electronic system not accounted for by the component analysis.

Table A3 - Calibration via Empirical White Noise Analysis

Factor	Value (dB)	
	709-90	710-90
Best-Fit Calibration Offset	-18.5	-18.5
FFT Size Adjustment (temporal)	-6.0	-12.0
FFT Size (spatial)	+24.1	+24.1
Hamming Shading (spatial)	-4.0	-4.0
TOTAL	-4.4	-10.4

The empirical frequency-dependent calibration curve could have been used, in principle, to correct for the system component rolloff at low frequencies. However, none of the attempted parameterizations of multiple high-pass filter models based on component values and/or best-fit values gave data calibrations that reproduced the frequency dependence of known experimental results below 250 Hz. As a result the experimental analysis was restricted to frequencies above 250 Hz for which the calibration was not expected to be strongly frequency dependent.

COMPARISON WITH EMPIRICAL CW ANALYSIS

An empirical analysis [A4] of the continuous-wave (CW) calibration Run 001 (709-90 Cruise Log No. 1, p. 23) was performed by Gary Gibian of Planning Systems, Inc. For this calibration a sine wave signal at 350 Hz was injected into the system. The input level at point B was measured to be -55.5 dBV/ $\sqrt{\text{Hz}}$. The output level from GENPASS was 155.6 dB. The effective hydrophone sensitivity (including the gain from the $\sqrt{10}$: 1 step-down transformer in the array itself) was taken as -204.4 dB re 1V/ μPa , giving a net calibration level of $-204.4 + (155.6 - (-55.5)) = +6.7$ dB.

To compare with the above calibration for the Cruise 709-90 ship-based data, appropriate adjustments must be included. The CW calibration beamforming used 23 hydrophones, giving a spatial FFT size adjustment of $10 \log[(16^2)/(23^2)] = -3.2$ dB. Uniform shading was used both spatially and temporally, so a -8.0 dB correction is needed to include the calibration for Hamming shading. The net calibration values from the empirical CW analysis are shown in Table A4.

Table A4 - Comparison with Empirical CW Analysis

Factor	Value (dB)
Empirical CW Calibration	+6.7
FFT Size (spatial)	-3.2
Hamming Shading	-8.0
TOTAL	-4.5

DATA CALIBRATION VALUES

The calibration finally applied to the data was an empirical curve similar to the three pole filter response curve. The actual values for the 709-90 data are shown in Table A5. Values for intermediate frequencies were obtained by linear interpolation. Values for the 710-90 data were 6 dB lower.

Comparison of the high frequency asymptotic calibration value of +0.5 dB with the component analysis value gives a difference of 1.3 dB, while comparison with the empirical white noise analysis value gives a difference of 4.9 dB. Comparison of the interpolated value for 350 Hz with the empirical CW analysis value gives a difference of approximately 2.4 dB.

Table A5 - Data Calibration Values

Frequency (Hz)	Value (dB)
256	-4.1
307	-2.9
358	-2.0
410	-1.5
461	-1.1
512	-0.8
563	-0.6
614	-0.4

ACKNOWLEDGMENTS

The authors gratefully acknowledge the assistance, help, and advice of Bruce Pasewark and Lilimar Avelino (NRL), as well as helpful discussions with Peter Ogden, Dennis Dundore, and David Drumheller (NRL) and with Gary Gibian (Planning Systems, Inc.).

REFERENCES

- A1. Bruce H. Pasewark, "Naval Research Laboratory Code 5160 Towed Array Specifications," NRL internal document (unpublished), 1987.
- A2. Steve Wolf, "Remarks on the Calibration of the Towed Array Amplifiers," NRL internal document (unpublished), 1982.
- A3. Steve Wolf, "Shallow-Water Towed Array Analog Signal Processing," NRL internal document (unpublished), 1982.
- A4. G. L. Gibian, "Calibration for 709-90 Run 202 CW Processing", NRL internal document, prepared by Planning Systems, Inc., (unpublished), 1991.

Appendix B

REPRESENTATIVE SOUND SPEED PROFILES

At each experimental site the *in situ* temperature profiles were measured using either expendable bathythermographs (XBTs) deployed from the side of the ship or airborne expendable bathythermographs (AXBTs) deployed from the P-3 aircraft. In addition, at the ship-based sites the surface water temperature was measured with a thermometer. The data were recorded and converted to sound speed using the SASEA software [B1]. At NRL the recorded sound speed data were edited, smoothed, and decimated using the SASEA software. For depths greater than approximately 1000 m these profiles were merged with archival profiles from the GDEM database [B2]. Plots of the resulting sound speed profiles are presented in Figs. B1, B2, and B3.

For the northernmost sites of Cruise 709-90 (Runs 709-1, 709-2, and 709-3) the channel axis was between 200 and 300 m, giving almost a duct environment and providing good ensonification of the surface. At the more southern sites the axis was deeper: For Run 709-4 the axis was around 600 m, while for Runs 709-5, 709-6, and 709-7 it was between 800 and 1000 m.

For Cruise 710-90 all the sites were clustered within approximately 90 km of each other. For these sites the channel axis was around 600 m. However, the Run 710-2 site was a notable exception, having a near duct profile with an axis around 100 m. Also, the Run 710-8 site appeared to show evidence of mixing within the first 200 m of the water column.

Among the airborne site sound speed profiles, the profiles at the northernmost sites (Flights c1, c2, and d, associated with 709-90) had axes between 200 and 400 m. The profiles for the southern sites (Flights f, g, h, and j, associated with 710-90) generally had axes around 600 m and also showed evidence of mixing within the first 200 m of the water column.

REFERENCES

- B1. Jeffery L. Hanson, "At-Sea Environmental Analysis - Valuable Tool for Oceanographic R&D," *Sea Technology*, **31** (2), 1990.
- B2. "Oceanographic and Atmospheric Master Library (OAML) Summary," OAML-SUM-21A, Naval Oceanographic Office, Stennis Space Center, MS, 1992.

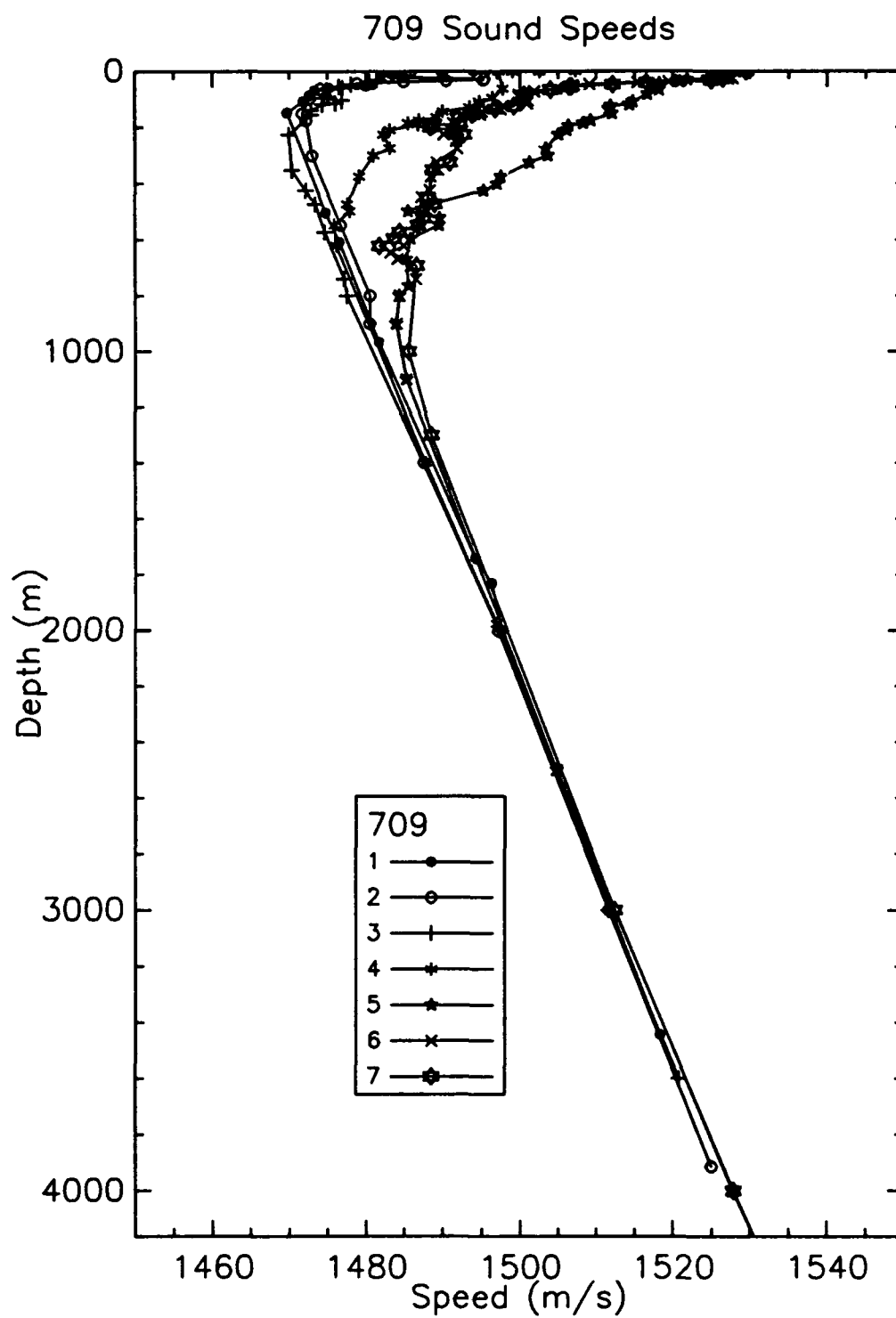


Fig. B1 – Representative sound speed profiles for the Cruise 709-90 experiment sites

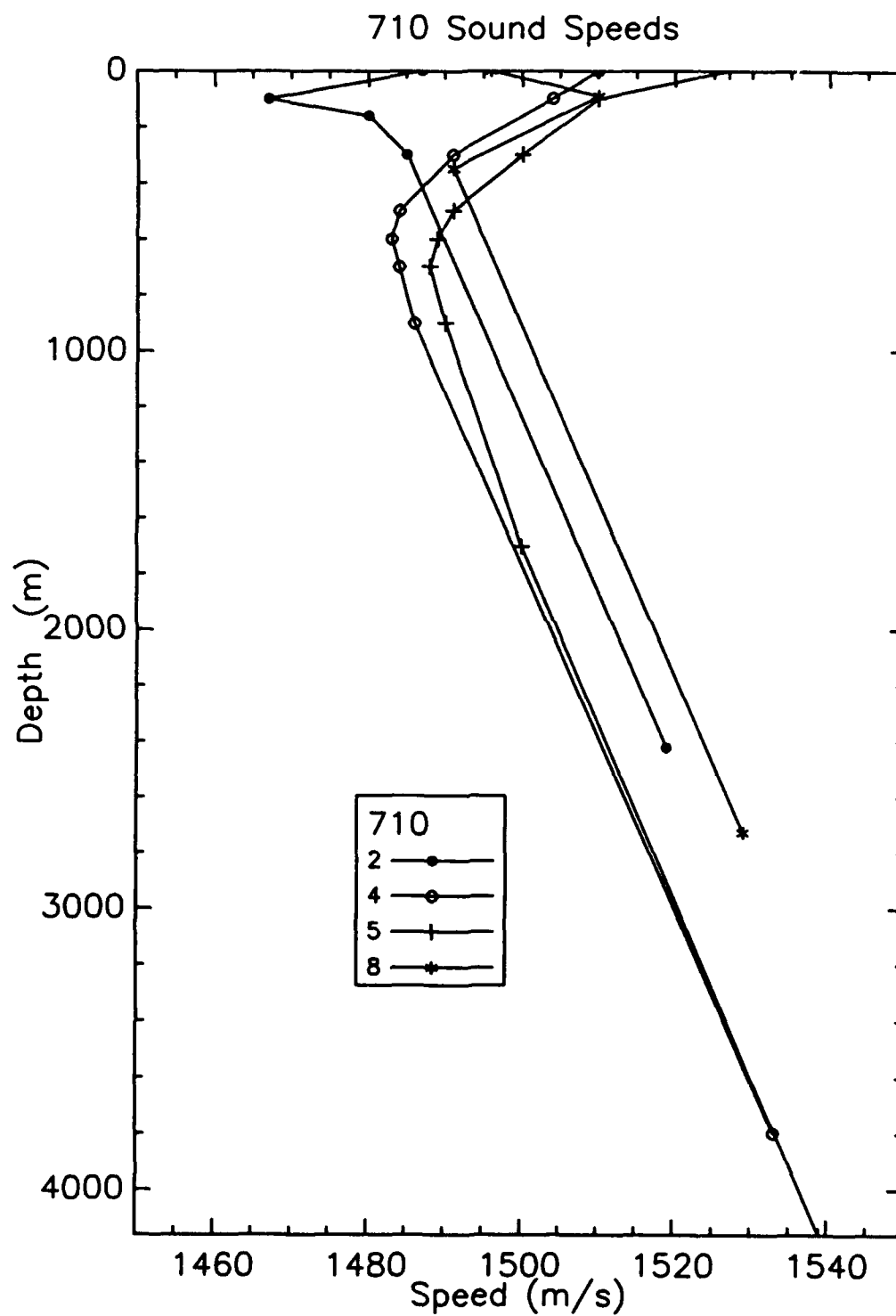


Fig. B2 - Representative sound speed profiles for the Cruise 710-90 experiment sites

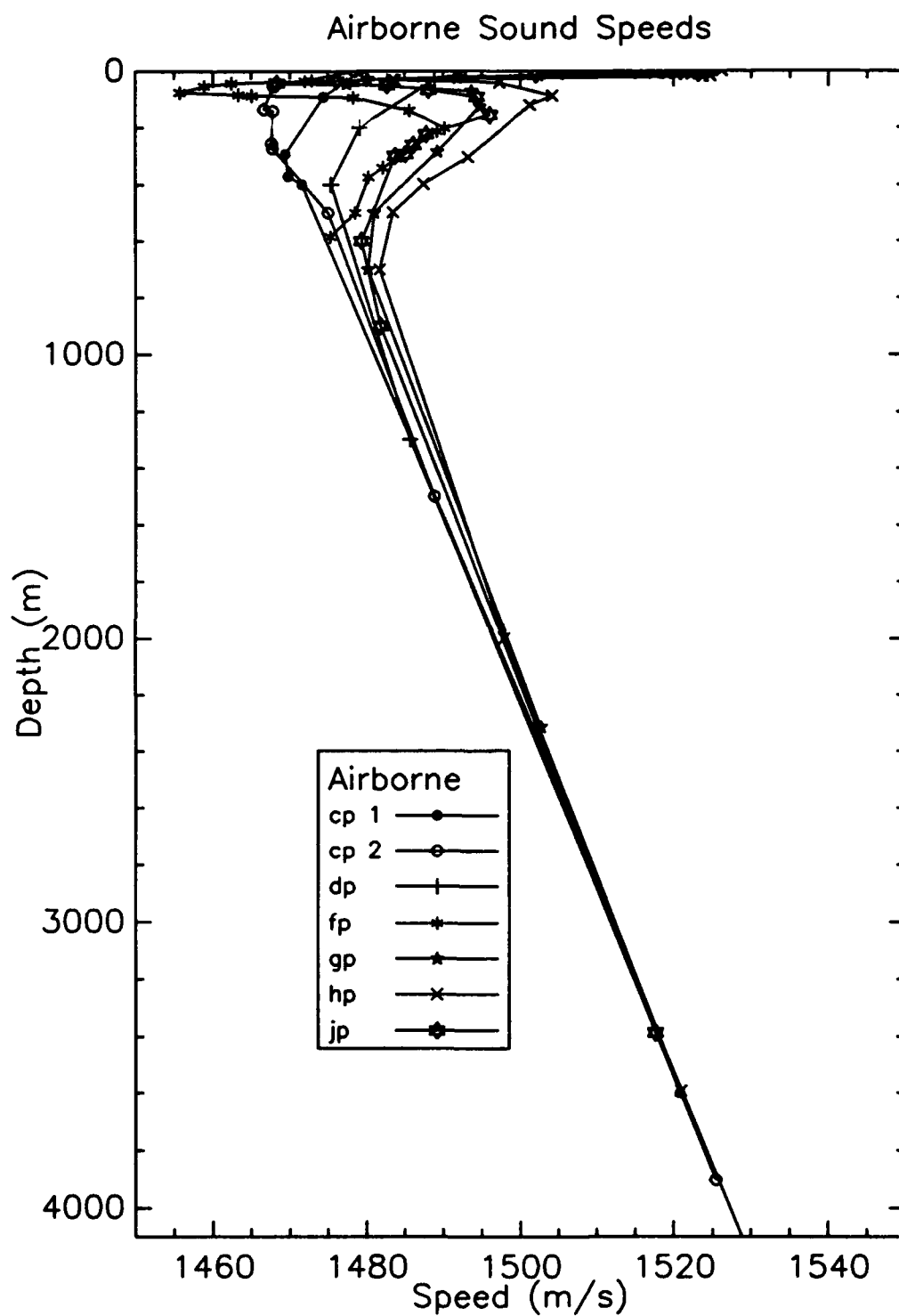


Fig. B3 - Representative sound speed profiles for the airborne experiment sites

Appendix C

3.5 KHZ ECHO SOUNDER PLOTS

The USNS *Lynch* had a 3.5 kHz echo sounder on board. This system transmitted bursts of sound at 3.5 kHz into the water and recorded the echo patterns on a chart recorder. The time delay of the echoes gave a direct measure of the bottom depth along the ship track. The echo patterns also contained implicit information about the properties of the upper portion of the seabed. Historically, this type of information has been used for empirical characterization of bottom types [C1]. However, because of arbitrary gain settings of the 3.5 kHz system on board the *Lynch*, the echo sounder chart recordings that were made were not of sufficiently high quality to enable extraction of echo character type.

Figures C1 to C11 present copy-reduced versions of the 3.5 kHz echo sounder chart recordings corresponding to the ship-based backscattering experiment runs. The ship speed was nominally 1.5 m/s, giving a nominal range rate of 2.7 km every half hour. The SUS charges were deployed typically between 3 and 5 min apart. The explosions of the SUS charges overloaded the echo sounder hydrophone and appeared on the chart recordings as vertical lines across the entire chart (e.g., see Fig. C6).

REFERENCE

- C1. E. P. Laine, J. E. Damuth, and Robert Jacobi, "Surficial sedimentary processes revealed by echo-character mapping in the western North Atlantic Ocean," in *The Geology of North America, Volume M, The Western North Atlantic Region*, P. R. Vogt and B. E. Tucholke, eds., The Geological Society of America, 1986.

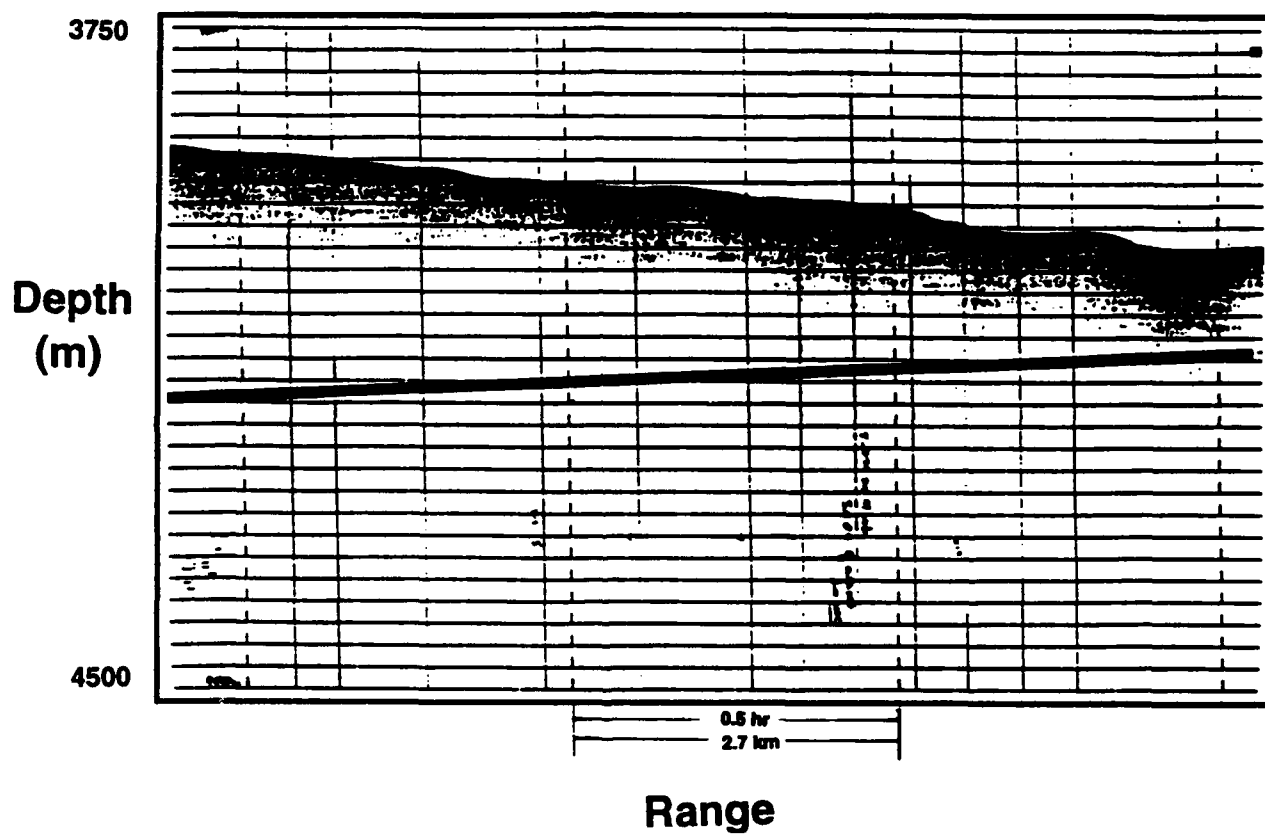


Fig. C1 - 3.5 kHz echo sounder plot for Run 709-1

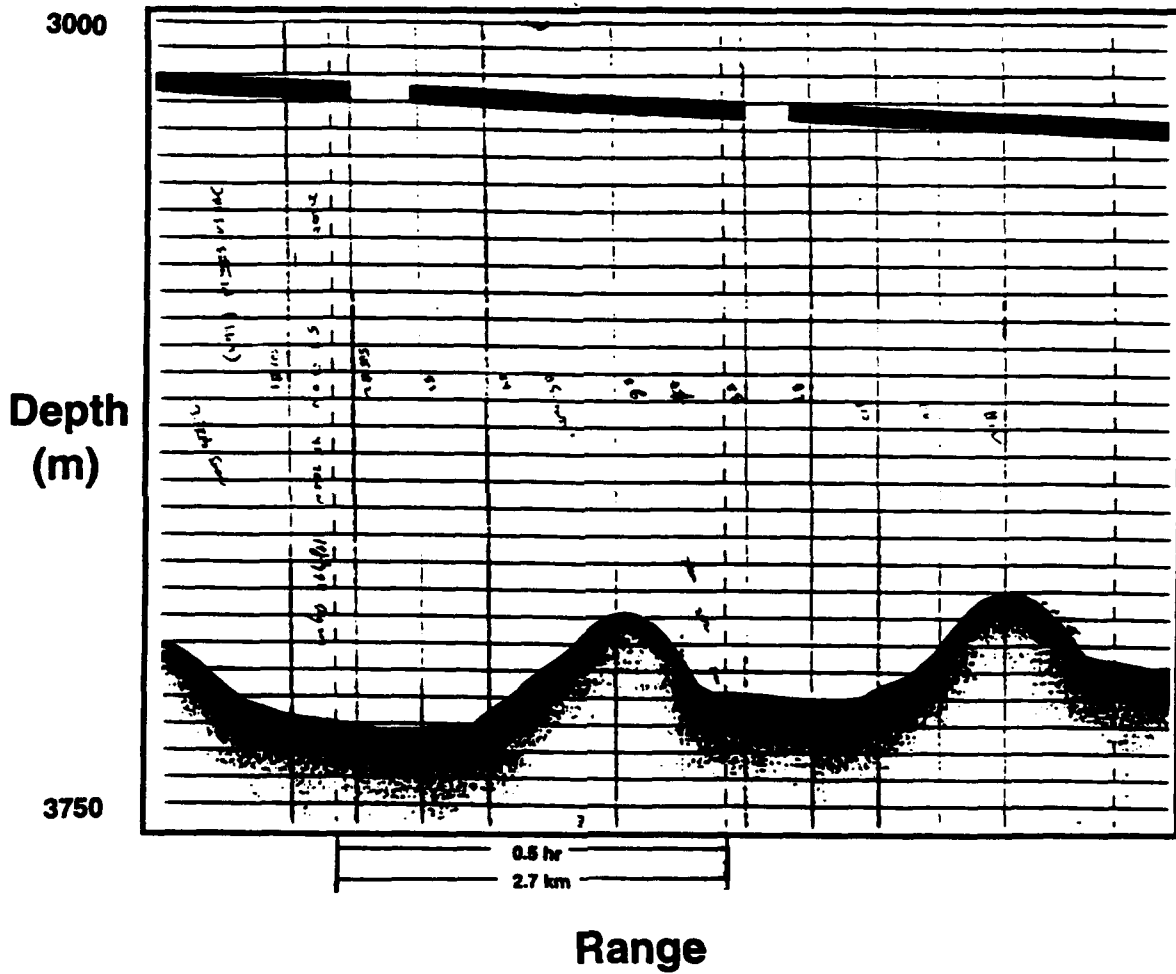


Fig. C2 - 3.5 kHz echo sounder plot for Run 709-2

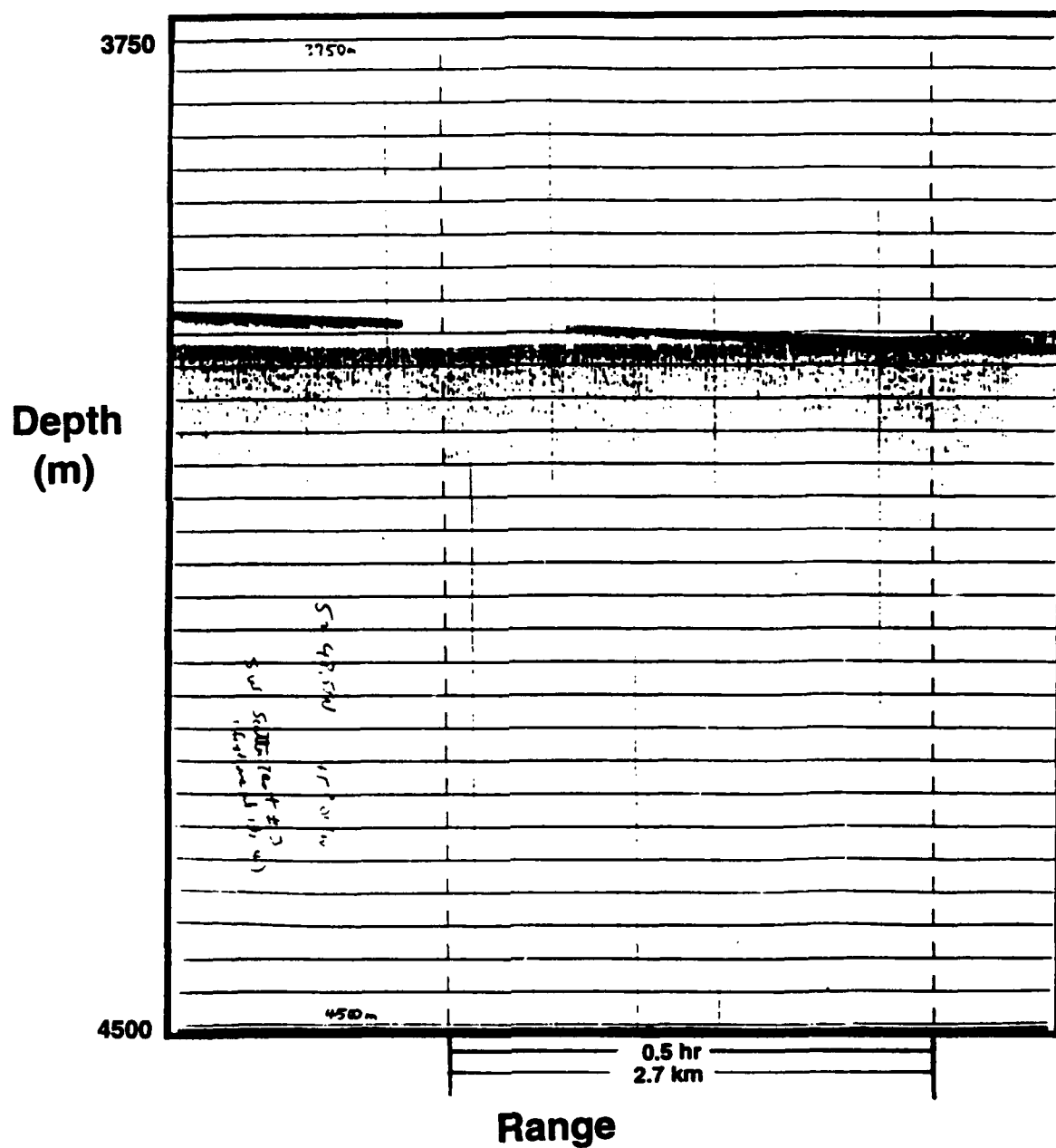


Fig. C3 - 3.5 kHz echo sounder plot for Run 709-3

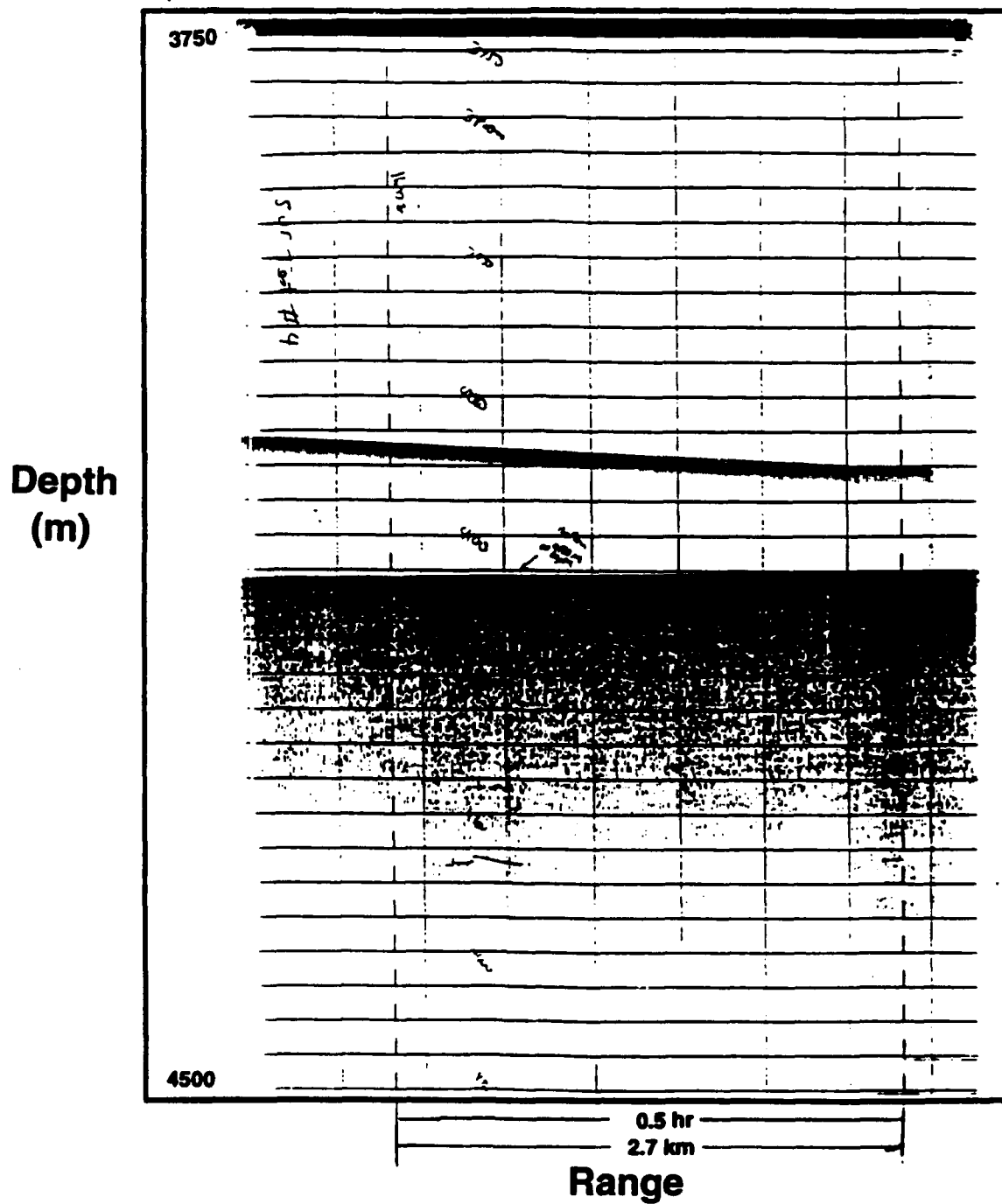


Fig. C4 - 3.5 kHz echo sounder plot for Run 709-4

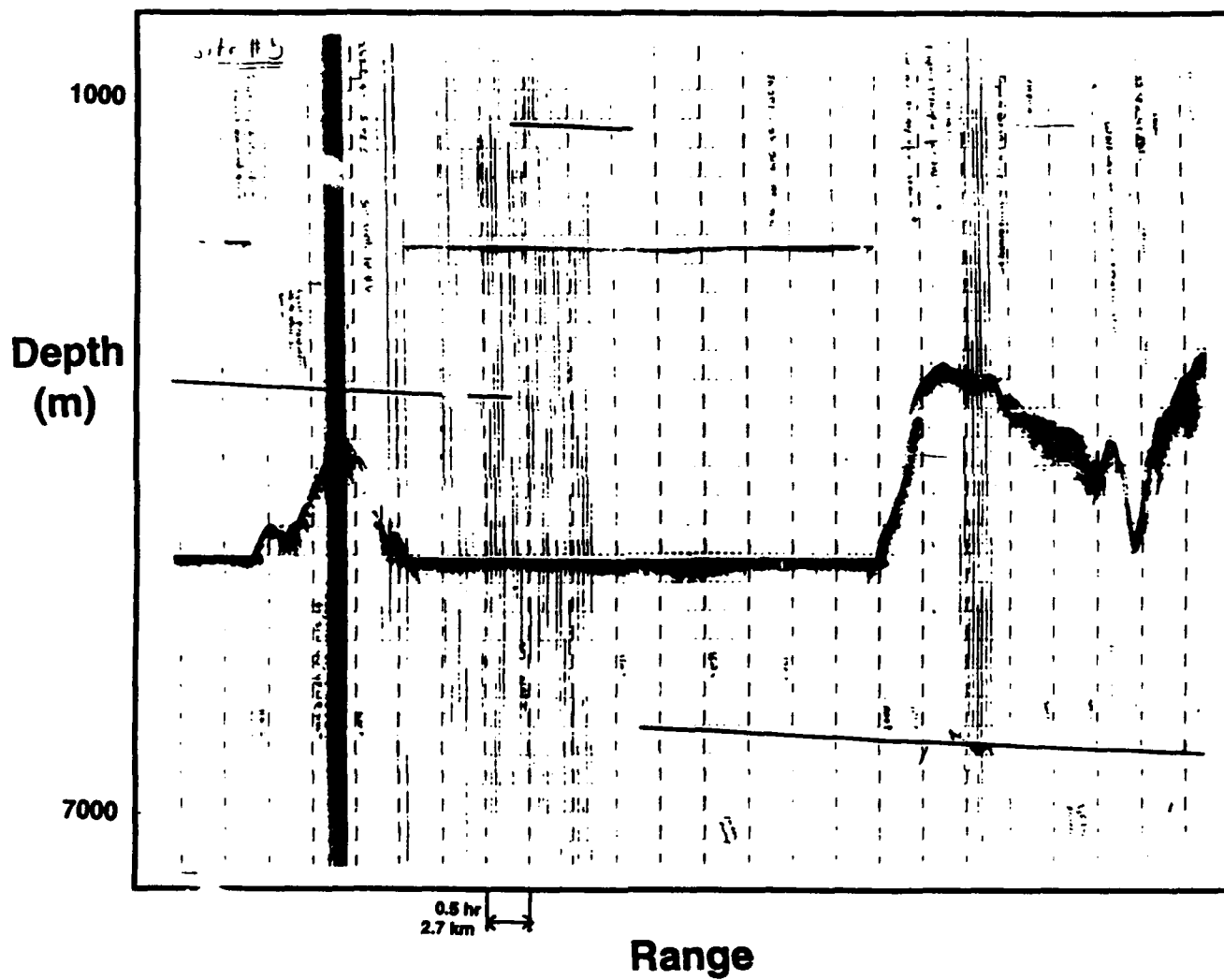


Fig. C6 - 3.5 kHz echo sounder plot for Run 709-6 and Run 709-7

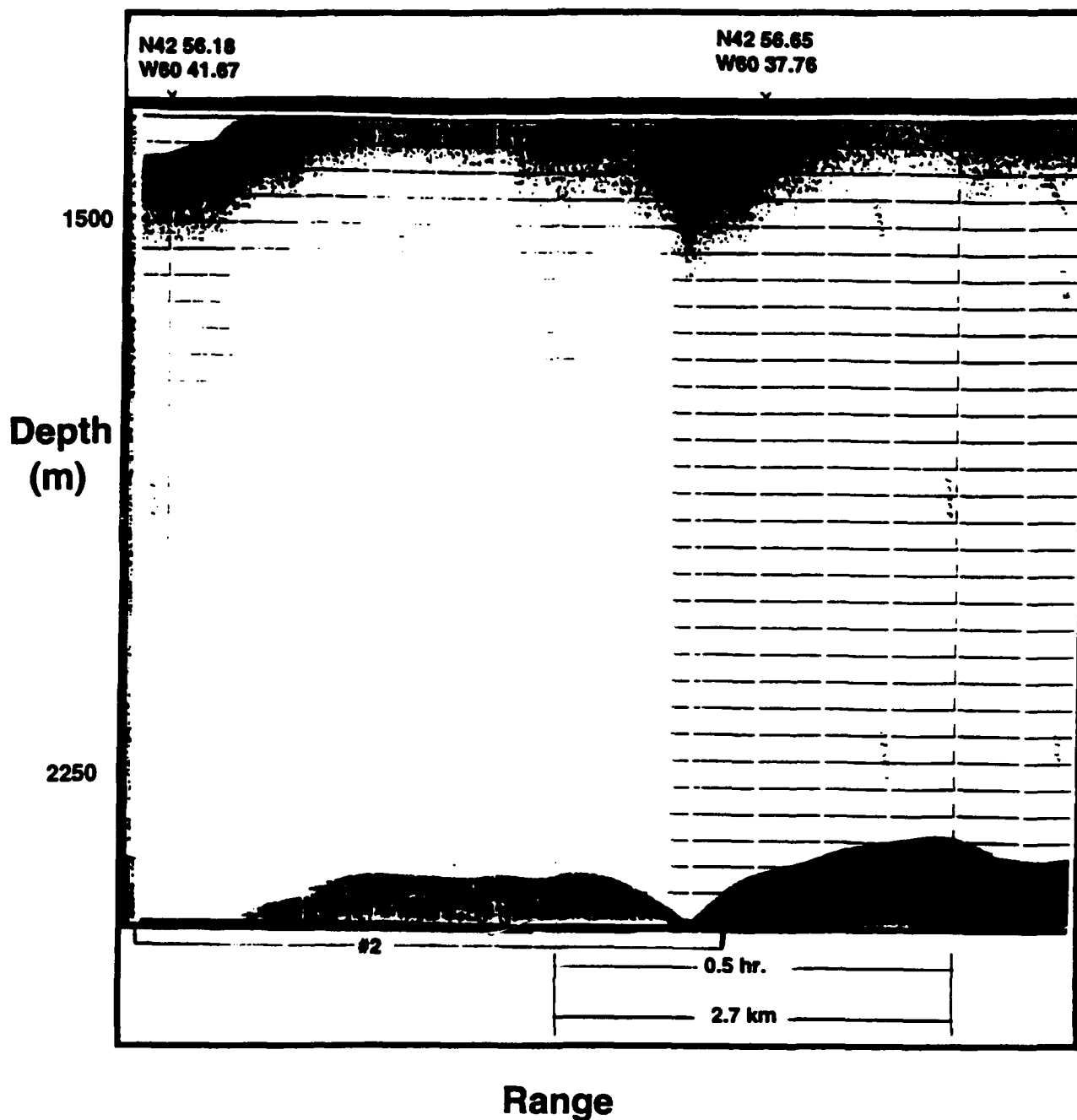


Fig. C7 - 3.5 kHz echo sounder plot for Run 710-2

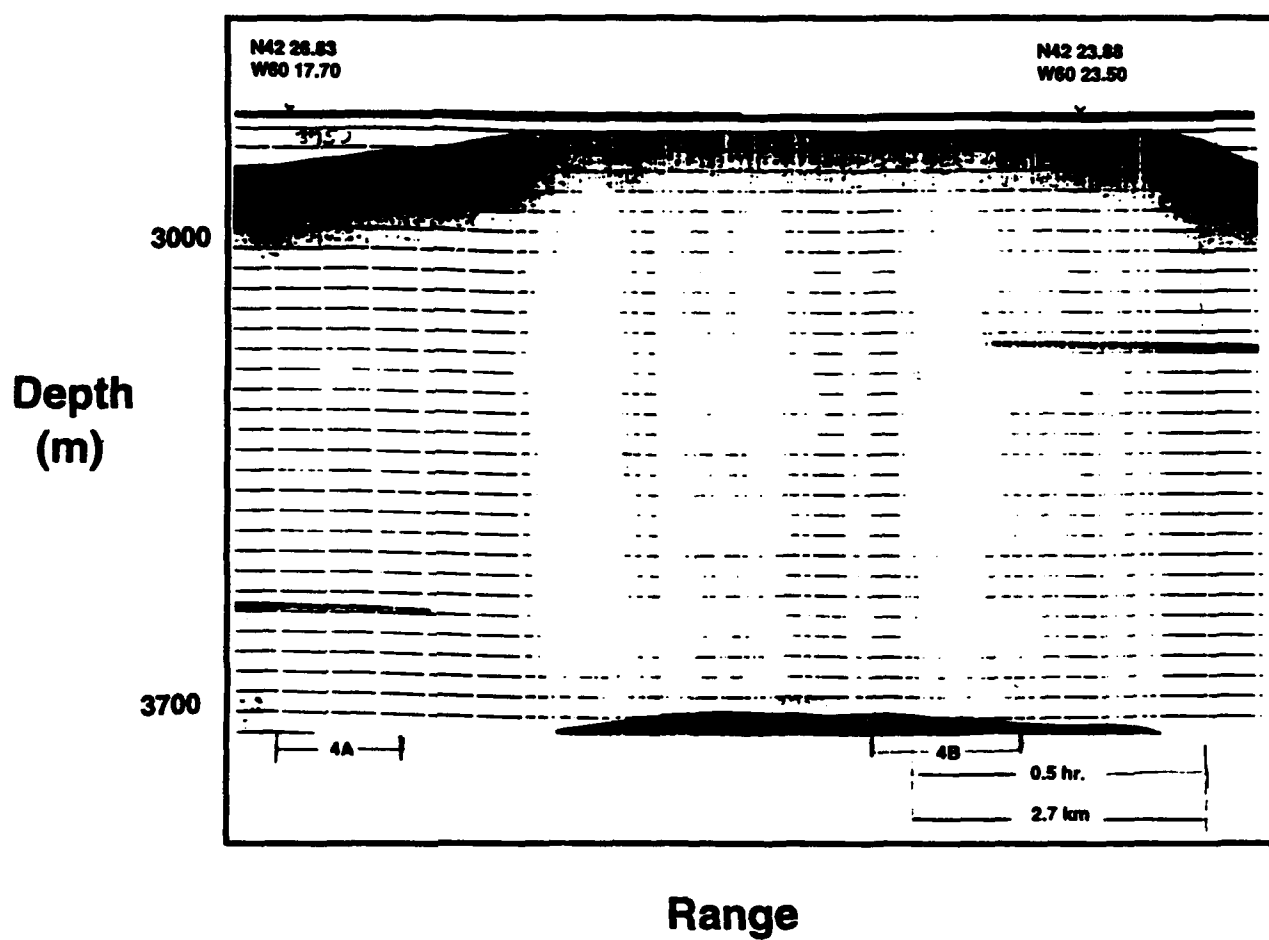


Fig. C8 - 3.5 kHz echo sounder plot for Run 710-4

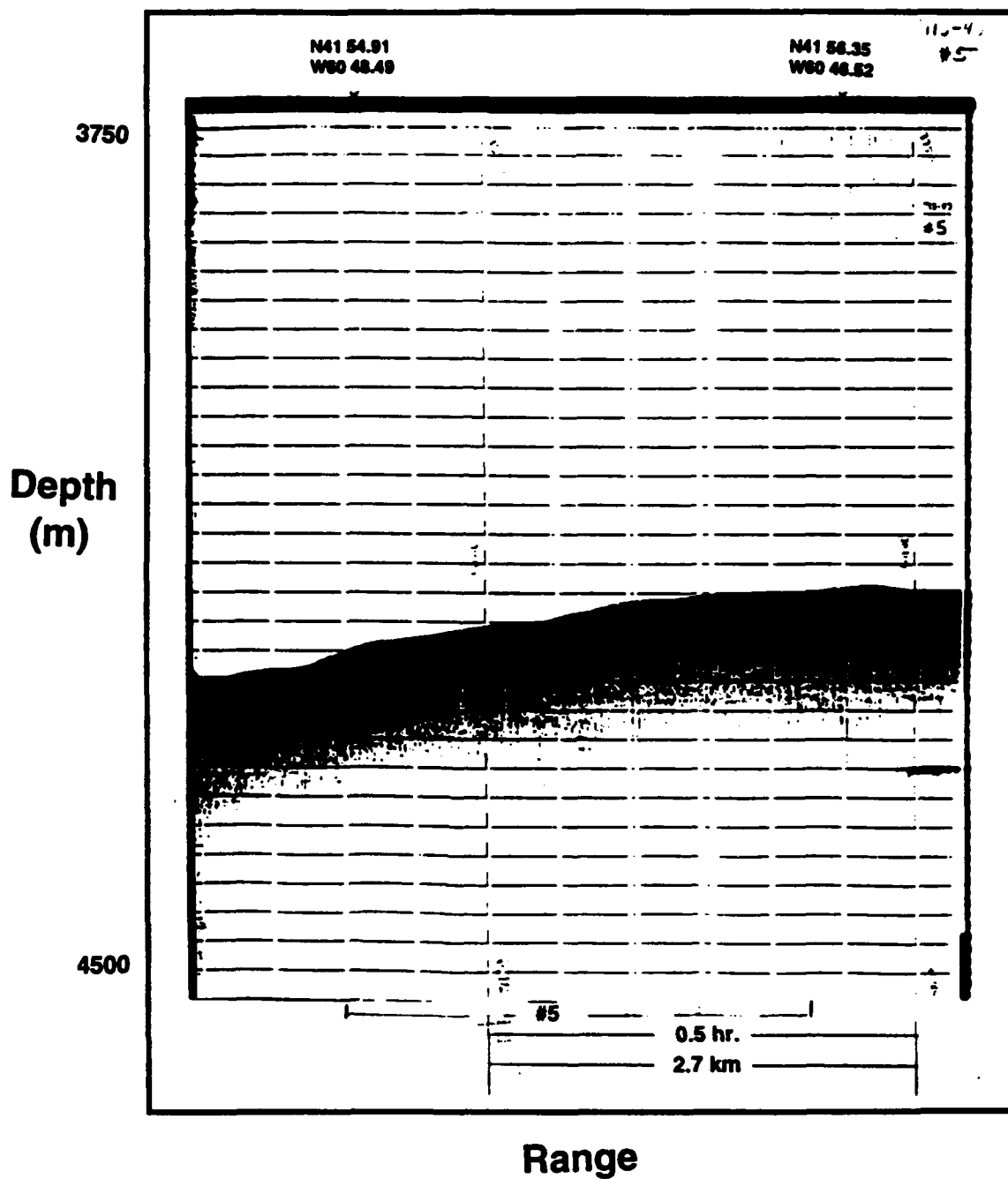


Fig. C9 - 3.5 kHz echo sounder plot for Run 710-5

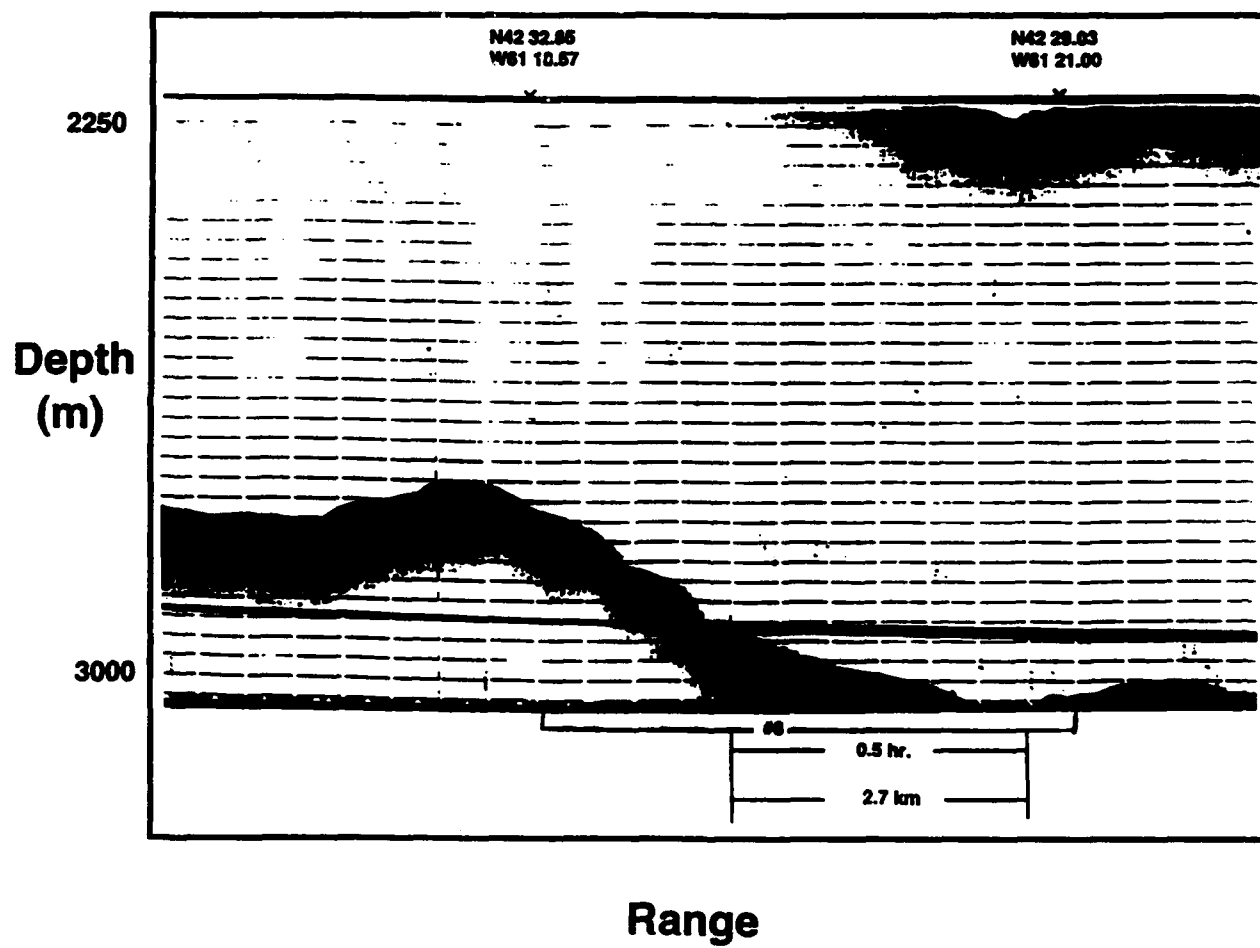


Fig. C10 - 3.5 kHz echo sounder plot for Run 710-8

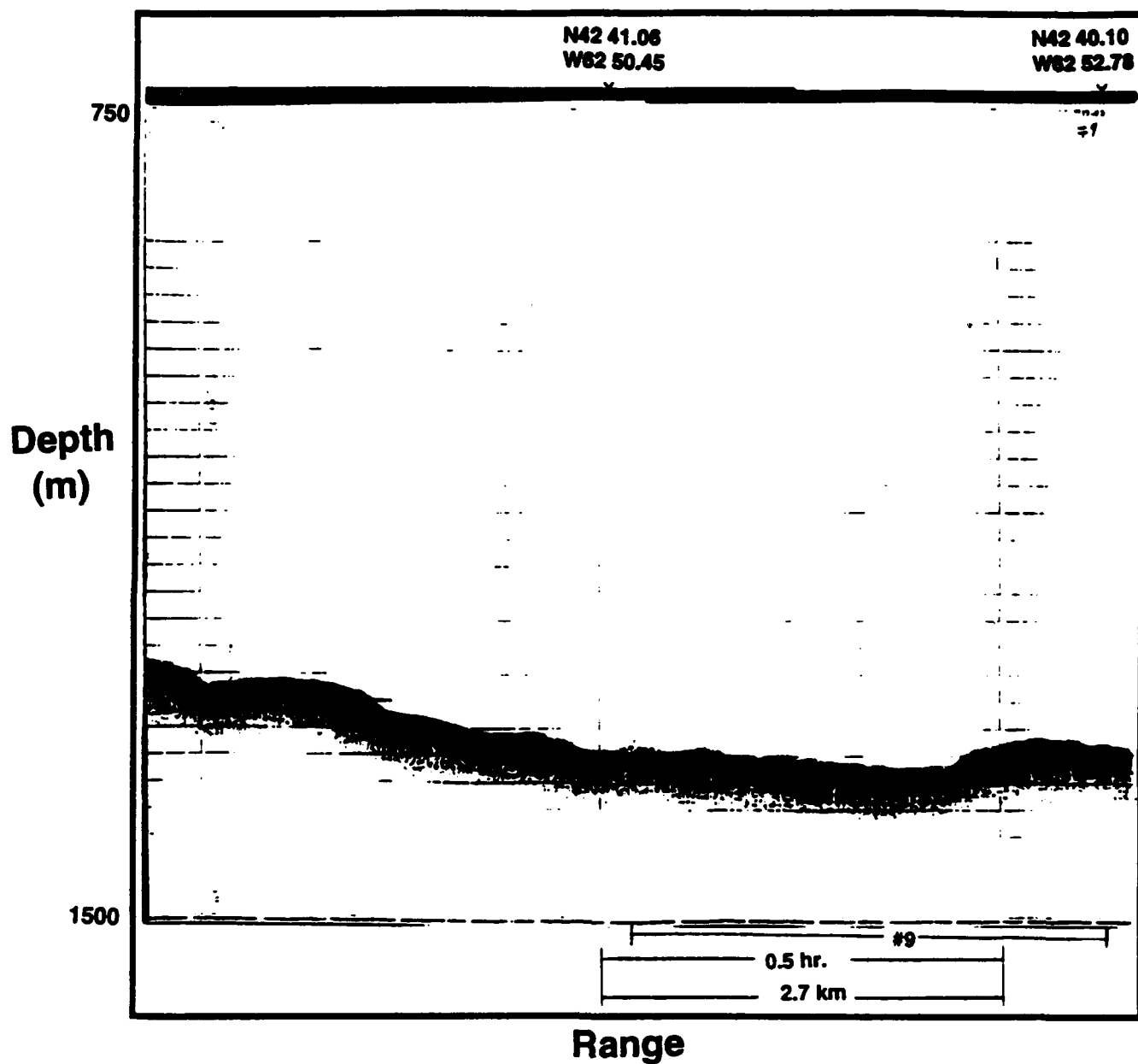


Fig. C11 - 3.5 kHz echo sounder plot for Run 710-9